Mohan, H., Friese, A., Albrecht, S., Krumbholz, M., Elliott, C. L., Arthur, A., Menon, R., Farina, C., Junker, A., Stadelmann, C., Barnett, S. C., Huitinga, I., Wekerle, H., Hohlfeld, R., Lassmann, H., Kuhlmann, T., Linington, C., and Meinl, E. (2014) Transcript profiling of different types of multiple sclerosis lesions yields FGF1 as a promoter of remyelination. Acta Neuropathologica Communications, 2, 178.

Copyright © 2014 The Authors.

This work is made available under the Creative Commons Attribution 4.0 International License (CC BY 4.0)

Version: Published

http://eprints.gla.ac.uk/104274/

Deposited on: 30 Mar 2015

Enlighten – Research publications by members of the University of Glasgow http://eprints.gla.ac.uk

Acta Neuropathologica Communications

BioMed Central
The Open Access Publisher

This Provisional PDF corresponds to the article as it appeared upon acceptance. Fully formatted PDF and full text (HTML) versions will be made available soon.

Transcript profiling of different types of multiple sclerosis lesions yields FGF1 as a promoter of remyelination

Acta Neuropathologica Communications 2014, **2**:168 doi:10.1186/s40478-014-0168-9

Hema Mohan (hema.mohan@ukmuenster.de)
Anita Friese (anita.friese@web.de)
Stefanie Albrecht (stefanie.albrecht@ukmuenster.de)
Markus Krumbholz (markus.krumbholz@med.uni-muenchen.de)
Christina L Elliott (Christina.Elliott@glasgow.ac.uk)
Ariel Arthur (ariel.arthur@gmail.com)
Ramesh Menon (menon.ramesh@hsr.it)
Cinthia Farina (farina.cinthia@hsr.it)
Andreas Junker (andreas.junker@med.uni-goettingen.de)
Christine Stadelmann (cstadelmann@med.uni-goettingen.de)
Susan C Barnett (Susan.Barnett@glasgow.ac.uk)
Inge Huitinga (i.huitinga@nin.knaw.nl)
Hartmut Wekerle (Hartmut.Wekerle@med.uni-muenchen.de)
Reinhard Hohlfeld (Reinhard.Hohlfeld@med.uni-muenchen.de)
Hans Lassmann (hans.lassmann@meduniwien.ac.at)
Tanja Kuhlmann (Tanja.Kuhlmann@ukmuenster.de)
Chris Linington (Christopher.Linington@glasgow.ac.uk)
Edgar Meinl (edgar.meinl@med.uni-muenchen.de)

Published online: 11 December 2014

ISSN	2051-5960
Article type	Research Article
Submission date	22 November 2014
Acceptance date	25 November 2014
Article URL	http://www.actaneurocomms.org/content/2/1/168

Like all articles in BMC journals, this peer-reviewed article can be downloaded, printed and distributed freely for any purposes (see copyright notice below).

Articles in BMC journals are listed in PubMed and archived at PubMed Central.

For information about publishing your research in BMC journals or any BioMed Central journal, go to http://www.biomedcentral.com/info/authors/

© Mohan et al,; licensee BioMed Central Ltd.
This is an Open Access article distributed under the terms of the Creative Commons Attribution License (http://creativecommons.org/licenses/by/4.0), which permits unrestricted use, distribution, and reproduction in any medium, provided the original work is properly credited. The Creative Commons Public Domain Dedication waiver (http://creativecommons.org/publicdomain/zero/1.0/) applies to the data made available in this article, unless otherwise stated.

Transcript profiling of different types of multiple sclerosis lesions yields FGF1 as a promoter of remyelination

Hema Mohan[1,8,10,†]
Email: hema.mohan@ukmuenster.de

Anita Friese[1,†]
Email: anita.friese@web.de

Stefanie Albrecht[2,†]
Email: stefanie.albrecht@ukmuenster.de

Markus Krumbholz[1,†]
Email: markus.krumbholz@med.uni-muenchen.de

Christina L Elliott[3]
Email: Christina.Elliott@glasgow.ac.uk

Ariel Arthur[3]
Email: ariel.arthur@gmail.com

Ramesh Menon[4]
Email: menon.ramesh@hsr.it

Cinthia Farina[4]
Email: farina.cinthia@hsr.it

Andreas Junker[5]
Email: andreas.junker@med.uni-goettingen.de

Christine Stadelmann[5]
Email: cstadelmann@med.uni-goettingen.de

Susan C Barnett[3]
Email: Susan.Barnett@glasgow.ac.uk

Inge Huitinga[6]
Email: i.huitinga@nin.knaw.nl

Hartmut Wekerle[7]
Email: Hartmut.Wekerle@med.uni-muenchen.de

Reinhard Hohlfeld[1,8]
Email: Reinhard.Hohlfeld@med.uni-muenchen.de

Hans Lassmann[9]
Email: hans.lassmann@meduniwien.ac.at

Tanja Kuhlmann[2]
Email: Tanja.Kuhlmann@ukmuenster.de

Chris Linington[3]
Email: Christopher.Linington@glasgow.ac.uk

Edgar Meinl[1*]
[*] Corresponding author
Email: edgar.meinl@med.uni-muenchen.de

[1] Institute of Clinical Neuroimmunology, Ludwig Maximilian University Munich, Max-Lebsche-Platz 31, D-81377 Munich, Germany

[2] Institute of Neuropathology, University Hospital Münster, Münster, Germany

[3] Division of Clinical Neurosciences, University of Glasgow, Glasgow, UK

[4] Division of Neuroscience, Institute of Experimental Neurology (INSpe), San Raffaele Scientific Institute, Milan, Italy

[5] Institute for Neuropathology, Göttingen, Germany

[6] The Netherlands Brain Bank, Netherlands Institute for Neuroscience, Amsterdam, Netherlands

[7] Max Planck Institute of Neurobiology, Hertie Senior Professorship, Martinsried, Germany

[8] Munich Cluster for Systems Neurology (SyNergy), Munich, Germany

[9] Center for Brain Research, Medical University of Vienna, Vienna, Austria

[10] Present address: Department of Neurology, University of Münster, Münster, Germany

[†] Equal contributors.

Abstract

Chronic demyelination is a pathological hallmark of multiple sclerosis (MS). Only a minority of MS lesions remyelinates completely. Enhancing remyelination is, therefore, a major aim of future MS therapies. Here we took a novel approach to identify factors that may inhibit or support endogenous remyelination in MS. We dissected remyelinated, demyelinated active, and demyelinated inactive white matter MS lesions, and compared transcript levels of myelination and inflammation-related genes using quantitative PCR on customized TaqMan Low Density Arrays. In remyelinated lesions, fibroblast growth factor (*FGF) 1* was the most abundant of all analyzed myelination-regulating factors, showed a trend towards higher expression as compared to demyelinated lesions and was significantly higher than in control white matter. Two MS tissue blocks comprised lesions with adjacent de- and remyelinated

areas and *FGF1* expression was higher in the remyelinated rim compared to the demyelinated lesion core. In functional experiments, FGF1 accelerated developmental myelination in dissociated mixed cultures and promoted remyelination in slice cultures, whereas it decelerated differentiation of purified primary oligodendrocytes, suggesting that promotion of remyelination by FGF1 is based on an indirect mechanism. The analysis of human astrocyte responses to FGF1 by genome wide expression profiling showed that FGF1 induced the expression of the chemokine *CXCL8* and leukemia inhibitory factor, two factors implicated in recruitment of oligodendrocytes and promotion of remyelination. Together, this study presents a transcript profiling of remyelinated MS lesions and identified FGF1 as a promoter of remyelination. Modulation of FGF family members might improve myelin repair in MS.

Keywords

Multiple sclerosis, Remyelination, Demyelination, Fibroblast growth factor

Introduction

The adult central nervous system contains a large pool of mitotic oligodendroglial progenitor cells (OPCs) which rapidly differentiate and remyelinate lesions in models of toxin or immune mediated demyelination [1]. In MS, however, this endogenous repair mechanism frequently fails, resulting in the formation of chronic demyelinated plaques with glial scars, the pathological hallmark of the disease [2,3]. This has profound functional consequences as demyelination not only disrupts saltatory conduction, but also compromises axonal survival by enhancing susceptibility to damage by inflammatory mediators [4], and by disrupting trophic support provided by myelinating oligodendrocytes [5-7]. The frequently observed failure of remyelination in MS does not appear to be due to an intrinsic, absolute defect of myelination, because de- and remyelinated MS lesions are frequently found side by side in the majority of patients. Furthermore, early MS lesions often show signs of remyelination [8-12].

It is unclear why many MS lesions fail to remyelinate. The presence of OPCs and premyelinating oligodendrocytes in many demyelinated lesions [13,14] suggests that this could be caused by failure of OPC to differentiate into myelinating oligodendrocytes. Overcoming this differentiation block to enhance remyelination by endogenous OPC is considered a logical strategy to restore saltatory conduction and reduce accumulation of disability due to axonal pathology [15,16]. Achieving this goal, however, is complicated as a multitude of cellular and molecular changes within the MS lesions can influence OPC migration, survival or differentiation [17-19]. While experimental studies demonstrate that many factors can individually influence OPC migration and/or differentiation [20-32], their relative expression within MS lesions and their significance in modulating remyelination remains unclear. Expression profiling of MS lesions can provide new insight into pathomechanisms [33-35], but this approach has not been applied to remyelinated lesions yet.

To identify endogenous pathways that might be exploited to enhance remyelination we analyzed white matter lesions and used qPCR to focus on the expression of genes regulating oligodendrocytes. We compared dissected remyelinated lesions, actively demyelinating lesions, inactive demyelinated lesions and control white matter. This revealed an important role of the FGF family in the regulation of remyelination. The FGF family is known to regulate oligodendrocyte biology and myelin thickness [36-40], but its role in MS lesion

development is unclear. We found that among the analyzed myelination-regulating genes *FGF1* was the most abundant transcript in remyelinated lesions. In two lesions that contained a demyelinated core and a remyelinated rim, the *FGF1* transcript levels were higher in the remyelinated parts suggesting that the increased availability of FGF1 may support remyelination.

FGF1 has been reported to promote proliferation of glial precursors [41], but had so far not been linked to remyelination or its failure in MS. We employed a dissociated myelinating culture system [42-44], a remyelinating slice culture model [45,46], a pure oligodendrocyte culture, and genome wide expression profiling of astrocytes to deduce the functional relevance. This revealed that FGF1 promotes myelination as well as remyelination, presumably via an indirect mechanism. In astrocytes, FGF1 induced leukemia inhibitory factor *(LIF)* and the chemokine *CXCL8*, both implicated in the recruitment of oligodendrocytes and the promotion of remyelination. This suggests that also in vivo FGF1 stimulates astrocytes to release factors promoting remyelination and that selective modulation of FGF signaling pathways could provide a novel strategy to enhance remyelination in MS and other demyelinating diseases.

Materials and methods

Tissue samples

For mRNA expression analysis we used frozen autoptic tissue samples from the Netherlands Brain Bank, the UK MS Brain Bank, the NeuroResource tissue bank, UCL London, and the Department of Forensic Medicine, LMU Munich. Twelve tissue blocks from 9 MS patients contained 12 white matter lesions, two of them with a demyelinated core and a remyelinated rim. As control, we used 6 control tissue blocks from 4 healthy subjects without clinical or histological evidence of CNS disease (details in Additional file 1: Table S1).

For immunostaining of FGF1 we used 10 formalin fixed paraffin embedded (FFPE) tissue blocks from 7 MS patients containing remyelinated, demyelinated inactive and demyelinated active areas as well as and 3 control tissue blocks form 3 healthy subjects. Most of the patients had secondary progressive MS. The mean disease duration was 24 years, the sex (f/m) ratio was 2:1 (details in Additional file 1: Table S1).

MS lesions were classified according to defined criteria: Active lesions contained abundant macrophages with degraded myelin products visualized by luxol fast blue (LFB) or oil red O staining. Inactive demyelinated lesions were sharply demarcated from the normal appearing white matter and largely devoid of macrophages. Remyelinated lesions were sharply demarcated from the normal appearing white matter and identified by a fainter LFB staining.

Tissue has been collected from donors from whom a written informed consent for brain autopsy and the use of the material and clinical information for research purposes.

Dissection of brain specimens, RNA extraction, cDNA synthesis, and quantitative PCR of brain tissue

Selected areas from tissue blocks were obtained as follows: Cryosections (20 µm) were mounted on PEN slides (P.A.L.M. Microlaser, Bernried, Germany). To identify demyelinated, remyelinated, control white matter, and grey matter areas every 6th section (30 µm) was stained with LFB. The unstained sections were superimposed on LFB stained sections and the lesion areas were marked and macrodissected manually. In total 200–300 µm of each block was used for transcript analysis. To check the precision of dissection, the macrodissected sections were stained with LFB. The control tissue samples used for qPCR exclusively contained white matter. Two MS tissue blocks with adjacent de-and remyelinated lesions were analyzed individually.

RNA was obtained from the dissected tissue specimens by guanidinium thiocyanate-phenol-chloroform extraction (TRI® Reagent, SIGMA, Munich, Germany), and cDNA was synthesized using random hexamers (High Capacity cDNA Reverse Transcription kit, Applied Biosystems (ABI, Darmstadt, Germany). Subsequently, qPCR was performed using custom made TaqMan Low Density Arrays (TLDAs) on the TaqMan 7900 thermocycler (both ABI). These TLDAs are based on qPCR reactions performed in 384 well plates with prespotted primers for the selected genes. We used the qPCR method for our study, because short amplicons (typically < 100 bp) give highly reliable expression data of autoptic tissue, both from frozen and in some cases even from FFPE material [47]. We included genes coding for factors regulating oligodendrocyte development (46), their receptors (20), myelin components (7) and genes that reflect immunological features of the lesions (9). The CNTF amplicon we quantified would also detect the ZFP91-CNTF read-through transcript which is thought to be non-coding (http://www.ncbi.nlm.nih.gov/gene/386607). Data were analyzed using RQ Manager 1.2 software (ABI). We applied three housekeeping genes, glyceraldehyde 3-phosphate dehydrogenase (*GAPDH*), β-actin (*ACTB*) and peptidylprolyl isomerase A *(PPIA)*. Differential gene expression was determined in 6 demyelinated inactive lesions from 4 subjects, 4 remyelinated lesions from 3 subjects, 4 demyelinated active lesions from 3 subjects, and 6 control white matter specimens from 4 subjects.

Histological stainings

To characterize the tissue lesions, conventional histochemical analysis like LFB and H&E, as well as immunohistochemistry for CD68 was used. LFB staining was done on 30 µm thick sections for frozen samples and on 4 µm for FFPE samples. Immunostaining for CD68 was performed with mouse peroxidase anti peroxidase (PAP) (Dako, Eching, Germany) system using diaminobenzidine (DAB) (DAKO) as the chromogenic substrate.

For FGF1 single staining with DAB, as well as the immunofluorescence staining, additional signal amplification was required. Tyramide signal amplification Plus Biotin kit (PerkinElmer, Waltham, USA) was used according to manufacturer instructions. To perform double staining, immunofluorescence was performed on FFPE sections. The sections (4 µm) were first deparaffinised and antigen retrieval was performed by boiling the slides for 30 min in Tris-EDTA buffer. To detect FGF1 we applied the mAb 2E12 (ab117640, Abcam, Cambridge, UK). This mAb recognizes FGF1 by Western blot, immunocytochemistry and flow cytometry, but we cannot exclude some crossreactivity to other FGF family members, since the epitope of this mAb has not yet been mapped (information from Abcam). Other primary antibodies used were specific for GFAP (Dako), Iba-1 (Wako, Neuss, Germany),

CD20 (Epitomics, Burlingame, USA) and CD3 (AbD Serotec, Kidlington, UK). Sections were incubated with the primary antibody either for 2 hours at RT or overnight at 4°C. The following secondary antibodies were used: goat anti-mouse IgG3 Alexa 488, goat anti-mouse IgG2a Alexa 488, goat anti-rabbit IgG Alexa 488 (Invitrogen, Karlsruhe, Germany), rat anti-mouse IgG1 biotinylated (BD, Heidelberg, Germany) and streptavidin Alexa 568 (Invitrogen) were used. Negative controls included either isotype specific antibody or the purified IgG.

All images were acquired on either Leica LMD7000 or Leica DMI6000 microscopes (Leica Microsystems, Wetzlar, Germany) and processed using ImageJ software (NIH).

In vitro myelination (dissociated spinal cord cultures)

In vitro myelinating cultures were prepared as described before [42-44]. Briefly, neurosphere derived astrocytes were grown to confluence. Spinal cord cell suspensions from either E15.5 Wistar or Sprague Dawley outbred rat strains were plated on the neurosphere derived astrocytes. The plating media contained 50% DMEM, 25% heat inactivated horse serum, 25% HBSS with Ca^{2+} and Mg^{2+}, and 2 mM L-glutamine. Spinal cord cells were plated in a density of 150,000 cells on a 13 mm cover slip, coated with poly-L-lysine. Cells were allowed to attach for 2 h at 37°C and subsequently, the plating medium was filled up with differentiation medium, containing DMEM (4.5 mg/ml glucose), 10 ng/ml biotin (Sigma), 0.5% N1 hormone mixture, 50 nM hydrocortisone, and 0.5 mg/ml insulin (Sigma). If not mentioned specifically, all the reagents used were from Invitrogen. The final ratio of plating- and differentiation-medium was 50/50. Three 13 mm coverslips were kept in 3.5 cm petri dishes with a total medium volume of 1 ml. Cultures were maintained at 37°C in7% CO_2 and fed three times a week by replacing half the culture medium with fresh differentiation media. After twelve day insulin was omitted from the culture medium. The cultures were maintained for 26–28 days (as indicated in the experiment). For stimulation recombinant human FGF1 was added together with fresh differentiation medium.

To access myelination immunocytochemistry was used. Briefly, cells were fixed with 4% PFA for 20 min at RT, washed in PBS and permeabilized with 0.5% Triton X-100 and 0.5% porcine gelatin for 20 min at RT. Primary antibodies used for the staining were specific for – neurofilament (SMI-31; Abcam), MBP (Millipore) or myelin oligodendrocyte glycoprotein (MOG). Secondary antibodies used were: Goat anti-mouse IgG2a Alexa 488 and goat anti-mouse IgG1 Alexa 568 (Molecular Probes). Primary antibodies were incubated overnight at 4°C. Secondary, fluorescence labeled antibodies were incubated for 45 min at room temperature and cover slips were mounted with Vectashield (Vector laboratories, Peterborough, UK).

For imaging and quantitative analysis 20–30 images per treatment per experiment were acquired at random with a 10X objective using ZEISS AxioVert200M or Olympus BX51 fluorescent microscope. For each condition 3 coverslips were quantified in each experiment. MBP and SMI-31 staining was measured as the pixel value related to the total pixel number in the image. The pixel values were calculated using either Metamorph software (series 7.7) or Image J (NIH systems, version 1.45) combined with Adobe Photoshop (Elements 7.0). To determine the percentage of myelination in each coverslip the number of MBP positive pixels was divided by the number of SMI-31 positive pixels. Significance of data values was analyzed using T-test.

Organotypic cerebellar slice cultures

Organotypic cerebellar slice cultures were prepared and cultured as previously described [48]. Briefly, cerebellum and attached hindbrain were extracted from newborn (P0) CD1 mouse pups (Charles River Laboratories) and cut into 300 µm sagittal sections using a McIlwain tissue chopper. Slices were separated and transferred on Millicell-CM culture inserts (Millipore, Darmstadt, Germany) in 6-well plates. Culture media was composed of 50% minimal essential media, 25% heat-inactivated horse serum, 25% Earle's balanced salt solution, 6.5 mg/ml glucose, and penicillin-streptomycin and Glutamax. Membranes were transferred into fresh media every 2–3 days. Slices were left untreated for 12 days *in vitro* to allow to myelinate [45]. Subsequently, slices were demyelinated with lysolecithin (0.5 mg/ml, 16 hours), washed in PBS and allowed to recover in culture media for 1 day. Afterwards, the slices were treated with FGF1 (100 ng/ml) for 7 days and 14 days, respectively. FGF1 was diluted in culture media and replaced every 2–3 days. Control slices remained untreated during the remyelination phase. Although these cultures are used to study remyelination, we are aware that they may still be equivalent of developmental myelination as the cultures were still at an ex vivo stage during which myelination is continuing in the in vivo cerebellum.

Total RNA from cultured cerebella slices were isolated using the RNeasy Micro Kit (Qiagen, Hilden, Germany) according to manufacturer's protocol. cDNA was generated using the High Capacity cDNA Transcription Kit (ABI). All qPCR analysis was conducted using the StepOne Plus real time cycler (ABI) and the Power SYBR Green Master Mix (ABI). All qPCR results were normalized to human acid ribosomal protein (*hARP*).

For immunostaining, slices were fixed in 4% PFA for 1 hour, and then washed twice in PBS. Subsequently the slices were blocked for 3 hours at room temperature. The primary antibody used recognized MBP (DAKO) and neurofilament (NFL) (DAKO). As secondary antibodies we used goat anti-rabbit Cy3 and goat anti-mouse Cy2 (Dianova, Germany). Primary antibody was incubated for 48 hours at 4°C, and the secondary, fluorescence labeled antibodies were incubated overnight at 4°C and the slices were mounted using Fluorescence Mounting Medium (DAKO).

From these, representative maximal-projection images were generated. The area ratio of MBP to NFL immunostaining was determined by drawing along only the filamentous structures per image and calculated the area using ImageJ. Per condition three animals were used for each of the three experiments.

Preparation of primary oligodendrocyte progenitor cells (OPCs)

Primary OPCs were isolated using the immunopanning method as described earlier [49]. Briefly, the dissected and chopped forebrains from P6 – P9 day old C57Bl/6 mice were incubated for 20 min at 37°C and 5 % CO_2 in papain buffer, titruated in ovomucoid solution (Cell Systems GmbH, Troisdorf, Germany) and centrifuged at 1000 rpm for 10 min. The cell pellet was resuspended in panning buffer and transferred to a negative selection plate coated with Anti-BSL 1 Griffonia simplificonia lectin (L-1100, Vector Labs/Biozol, Eching, Germany). The supernatant was transferred to a positive selection plate coated with rat anti-mouse CD140a (10R-CD140AMS, Research Diagnostics/Bioleague, Poggensee, Germany) as primary antibody and AffiniPure goat anti-rat IgG (H + L) (112-005-003, Dianova) as secondary antibody. After incubation the adherent OPCs were detached by using a cell

scraper, centrifuged for 10 min at 1000 rpm, resuspended in mouse OPC Sato media [49] and plated in T75 culture flask coated with poly-L-lysine. The OPCs were cultured at 37°C and 5 % CO_2; PDGF-AA (10 ng/ml, Peprotech) was added every day. Half of the media was changed every second or third day. The purity of the OPCs cultures was more than 95 %.

Assessment of oligodendroglial proliferation and differentiation

Proliferation of OPCs was determined using BrdU incorporation (Cell Proliferation ELISA, BrdU [colorimetric], Roche Diagnostics, Penzberg, Germany). Oligodendroglial differentiation was assessed by morphology. To allow differentiation of OPCs into oligodendrocytes, PDGF-AA was replaced by 10 ng/ml ciliary neurotrophic factor (CNTF) (Peprotech). Brightfield pictures were taken after 48 h. At least 100 cells per time point were classified as oligodendroglial progenitor (0–2 processes), immature (3–13 processes) or mature (differentiated cells with myelin sheet formation) oligodendrocytes.

RNA isolation and qRT-PCR from oligodendrocyte and slice cultures

Total RNA was isolated using peqGOLD Total RNA Kit and mRNA was transcribed into cDNA by reverse transcription reaction (High Capacity cDNA Transcription Kit, ABI). qRT-PCR was performed using Power SYBR® Green PCR Master Mix (ABI) and StepOne Plus real time cycler (ABI). The following primers were used: hARP forward 5’ CGACCTGGAAGTCCA-ACTAC 3’; hARP reverse 5’ ATCTGCTGCATCTGCTTG 3’; MBP for 5’ GTACAAG-GACTCACACACGAGA 3’; MBP rev 5’ GTTCGAGGTGTCACA ATGTTCT 3’; MAG for 5’ ACCGCCTTCAACCTGTCTGT 3’; MAG rev 5’ CTCGTT CACAGTCACGTTGC 3’; MOG for 5’ CCTGCAGCACAGACTGAGAGGAAAA 3’; MO G rev 5’ TGCTGGGC-TCTCCTTCCGCT 3’.

Primary astrocyte cell culture, genome wide transcriptome analysis and RT-qPCR analysis

Human astrocytes of embryonic origin [50] were cultured as described [51]. Medium was changed to serum-free Panserin 401 (PAN Biotech, Aidenbach, Germany) supplemented with 1 % penicillin-streptomycin 24 h prior to stimulation with recombinant human FGF1 (10 ng/ml; R&D Systems) and 5 U/ml Heparin-Natrium-25000-ratiopharm® (ratiopharm, Ulm, Germany). Astrocytes were stimulated for 8 or 24 hours with FGF1 + heparin or heparin alone. Triplicates were analysed for each timepoint. Total RNA from was extracted using RNeasy Mini Kit (Qiagen). 200 ng of total RNA was spiked with polyadenylated transcripts using the Gene Chip® Poly-A Control kit (Affymetrix, Santa Clara, USA). cRNA was generated and transcribed into anti-strand and strand cDNA. The strand cDNA was purified using the Ambion WT Expression kit (Life Technologies, Carlsbad, USA) and labeled with the Affymetrix GeneChip® WT Terminal Labeling and Control kit (Affymetrix, Santa Clara, USA).

Samples were hybridized to Affymetrix GeneChip® Human Gene 1.0 ST Arrays, containing about 29000 probesets representing annotated human transcripts present in NCBI-RefSeq database. The arrays were scanned using the GeneChip® 3000 scanner and the transcriptome data were exported using AGCC Scan Control software v3.2.3.1515. Subsequently data processing and analysis were performed in R/Bioconductor platform (www.bioconductor.org). The data were subjected to robust multi-array (RMA)

normalization [52]. Further, 26839 probesets passed detection above background (DABG) p-value < 0.05 in at least 25 % of the samples and were considered for the subsequent analysis. No outlier samples were identified by principal component analysis and unsupervised hierarchical clustering based on filtered genes. Differential expression analysis was performed using ebayes test followed by Benjamini&Hochberg method for multiple testing correction, as implemented in the LIMMA bioconductor package [53]. Differentially expressed probes were defined by three criteria: (a) corrected p-value <0.05, (b) fold change threshold ± 1.4 (c), normalized mean expression intensity > = 100 in any one of the two groups.

Reverse transcription qPCR was performed using TaqMan® assays (ABI) to quantify the expression of *HMOX1* (Hs01110250_m1), *CXCL8* (Hs00174103_m1), *LIF* (Hs00171455_m1), and *PPIA* (4326316E). TaqMan® PCR Core Reagent Kit (ABI) was applied, PCR was performed on the 7900HT Fast Real-Time PCR System (ABI) and SDS software version 2.3 (ABI) was used for data analysis.

ELISA

We used ELISA assays to detect human CXCL8 (#DY208) and human LIF (#DY7734-05) (R&D Systems). 3.3′,5.5′-Tetramethylbenzidine (TMB) solution (Sigma-Aldrich) was used as substrate and color reaction was stopped by adding 1 mol/l H_2SO_4. Absorption was measured at 450 nm and 540 nm.

Results

Astrocyte activation and immune cells in remyelinated lesions

CD68 and *HLA-DR* expression was highest in the active lesions (Table 1). Transcripts for myelin associated genes were greatly reduced in the demyelinated inactive lesions compared to remyelinated lesions (Table 1). The myelin associated genes, were however, not completely absent in demyelinated lesions (Table 1), an observation which can be explained by the presence of premyelinating oligodendrocytes in the demyelinated lesions [13]. A heat map of all analyzed de-and remyelinated lesions, which were dissected based on LFB staining, shows that our qPCR results reflected the established pathology of MS lesions (Additional file 2: Figure S1).

Table 1 Expression levels of myelin genes, astrocyte and inflammation markers in MS lesions and their fold changes in demyelinated inactive versus remyelinated lesions

Gene name	CWM		Remyelinated		Demyelinated		Active		*Re/CWM*		*Re/De*	
	mean	SEM	mean	SEM	mean	SEM	mean	SEM	*ratio*	p	*ratio*	p
Myelin proteins												
CNP	**333.38**	75.99	**539.31**	253.33	**50.77**	20.00	**228.49**	77.20	*1.62*	0.48	*10.62*	***0.0095***
MAG	**57.21**	10.00	**65.82**	11.80	**11.57**	6.28	**43.18**	4.67	*1.15*	0.76	*5.69*	***0.019***
MBP	**40.84**	7.40	**41.85**	13.02	**6.91**	2.49	**107.43**	83.98	*1.02*	0.76	*6.06*	***0.0095***
MOBP	**350.12**	84.65	**422.56**	164.85	**34.10**	18.05	**316.04**	145.56	*1.21*	0.91	*12.39*	***0.0095***
MOG	**61.33**	15.60	**90.21**	13.05	**10.87**	5.26	**50.26**	14.17	*1.47*	0.26	*8.30*	***0.0095***
OMG	**48.67**	13.67	**86.83**	32.00	**13.87**	4.27	**20.85**	4.88	*1.78*	0.35	*6.26*	***0.019***
PLP1	**2239.24**	486.85	**3434.69**	397.98.	**400.80**	143.30	**1917.75**	252.49	*1.53*	0.11	*8.57*	***0.0095***
Astrocyte and inflammation markers												
GFAP	**890.74**	123.37	**2713.08**	451.88	**4715.80**	1637.94	**11466.90**	9726.52	*3.05*	**0.010**	*0.58*	*0.91*
CD68	**5.57**	0.68	**11.24**	1.00	**12.07**	3.67	**62.60**	33.16	*2.02*	**0.010**	*0.93*	*1*
HLA-DRA	**21.83**	6.34	**29.63**	8.83	**20.66**	4.05	**79.79**	7.09	*1.36*	0.48	*1.43*	*0.35*
IL1B	**0.17**	0.02	**0.14**	0.06	**0.19**	0.10	**0.33**	0.12	*0.80*	0.76	*0.71*	*1*
IL10	**0.13**	0.03	**0.24**	0.06	**0.07**	0.03	**0.71**	0.40	*1.82*	0.26	*3.29*	***0.040***
TNFSF13B (BAFF)	**0.71**	0.17	**2.04**	0.64	**0.95**	0.27	**2.88**	1.10	*2.88*	0.067	*2.15*	*0.26*
TGFB1	**5.32**	0.99	**12.68**	2.10	**15.03**	6.22	**106.86**	97.86	*2.38*	**0.010**	*0.84*	*1*
TGFB2	**2.02**	0.16	**5.08**	0.86	**7.35**	2.66	**5.36**	0.63	*2.52*	**0.010**	*0.69*	*0.76*
TGFB3	**4.73**	0.70	**9.75**	4.75	**3.09**	0.77	**8.10**	5.37	*2.06*	0.35	*3.15*	*0.067*

CWM: Control white matter, Remyelinated: Remyelinated lesion, Demyelinated: Demyelinated inactive lesion, Active: Demyelinated active lesion, Re/CWM and De/Re ratio: Remyelinated vs. control white matter and vs. demyelinated inactive lesions, respectively; p value were calculated by 2-sided U tests, unadjusted for multiple testing. p-values < 0.05 are printed in bold. Specimens analyzed: Six normal white matter specimens from 4 subjects, 6 demyelinated inactive lesions from 4 subjects, 4 demyelinated active lesions from 3 subjects, and 4 remyelinated lesions from 3 subjects were dissected and used for qPCR analysis. The mean expression values are given as % *GAPDH*; SEM denotes standard error of the mean.

In remyelinated lesions, glial fibrillary acidic protein (*GFAP*) was significantly higher expressed than in control white matter, indicating a persistent astrocytic activation in the presence of repaired myelin (Table 1). *CD68*, a marker for microglia activation and macrophage infiltration was also significantly elevated in remyelinated lesions (Table 1). B cell activating factor of the TNF family (*BAFF*), a B cell survival factor was also high in remyelinated lesions (Table 1), which might reflect the persisting astrocytic activation [51].

Altered expression of oligodendrocyte regulators in de- and remyelinated MS lesions

We quantified the expression of mediators regulating oligodendrocytes focusing on semaphorins, FGFs, PDGFs, chemokines, IL-6 and IGF family members (Table 2) as well as their receptors in the three different lesion types and control white matter (Additional file 3: Table S2).

Table 2 Expression levels of genes potentially regulating oligodendrocytes and their fold changes in demyelinated inactive versus remyelinated lesions

Gene name	CWM		Remyelinated		Demyelinated		Active		*Re/CWMl*		*Re/De*	
	mean	**SEM**	**mean**	**SEM**	**mean**	**SEM**	**mean**	**SEM**	***ratio***	**p**	***ratio***	**p**
PDGFs												
PDGFA	**19.38**	2.59	**31.78**	10.91	**15.45**	4.47	**51.82**	34.22	*1.64*	0.61	*2.06*	*0.26*
PDGFB	**1.23**	0.28	**1.71**	0.30	**6.79**	2.91	**31.65**	29.42	*1.39*	0.26	*0.25*	*0.48*
PDGFC	**0.52**	0.09	**1.45**	0.47	**1.19**	0.48	**2.56**	1.69	*2.78*	**0.038**	*1.22*	*0.61*
PDGFD	**0.14**	0.05	**0.37**	0.22	**0.83**	0.46	**0.08**	0.03	*2.61*	1.00	*0.45*	*0.45*
FGFs												
FGF1	**39.42**	2.61	**85.40**	11.54	**48.15**	19.53	**58.18**	16.80	*2.17*	**0.010**	*1.77*	*0.11*
FGF2	**3.82**	0.56	**9.23**	0.88	**10.25**	2.62	**6.08**	0.63	*2.41*	**0.010**	*0.90*	*0.91*
FGF5	**0.01**	0.01	**0.00**	0.00	**0.01**	0.01	**0.00**	0.00	*0.00**	0.15	*0.00**	*0.15*
FGF8	**0.00**	0.00	**0.06**	0.05	**0.02**	0.01	**0.01**	0.00	*16.25**	0.74	*2.69**	*0.72*
FGF9	**0.04**	0.02	**0.02**	0.01	**0.87**	0.53	**0.01**	0.00	*0.44**	0.71	*0.02**	*0.066*
Semaphorins												
SEMA3A	**0.58**	0.11	**0.77**	0.10	**1.77**	0.75	**0.71**	0.25	*1.32*	0.26	*0.43*	*0.35*
SEMA3B	**6.33**	1.73	**10.48**	4.21	**2.82**	1.50	**5.37**	3.57	*1.66*	0.61	*3.72*	*0.11*
SEMA3C	**4.84**	1.06	**7.13**	0.75	**2.10**	0.59	**6.13**	1.73	*1.47*	0.17	*3.40*	***0.010***
SEMA3D	**0.55**	0.09	**2.18**	0.57	**1.08**	0.37	**0.85**	0.23	*3.94*	**0.019**	*2.02*	*0.11*
SEMA3E	**0.41**	0.04	**0.91**	0.29	**0.49**	0.15	**0.69**	0.23	*2.21*	0.26	*1.84*	*0.17*
SEMA3F	**0.02**	0.01	**0.02**	0.01	**0.20**	0.10	**1.91**	1.89	*0.93**	0.91	*0.10**	*0.44*
SEMA3G	**0.23**	0.05	**0.16**	0.06	**0.54**	0.31	**1.18**	0.98	*0.68*	0.48	*0.30*	*0.91*
SEMA4A	**0.22**	0.06	**0.21**	0.05	**1.00**	0.36	**0.29**	0.04	*0.95*	0.91	*0.21*	*0.067*
SEMA4B	**2.63**	0.31	**8.90**	2.16	**8.46**	3.46	**18.31**	14.74	*3.39*	**0.010**	*1.05*	*0.48*
SEMA4C	**4.49**	0.77	**8.07**	2.81	**3.67**	0.83	**9.90**	6.17	*1.80*	0.26	*2.20*	*0.11*
SEMA4D	**16.61**	3.51	**24.36**	7.25	**4.72**	2.38	**23.80**	11.36	*1.47*	0.61	*5.16*	***0.019***
SEMA4F	**0.40**	0.04	**1.27**	0.13	**3.09**	0.67	**4.83**	4.19	*3.18*	**0.010**	*0.41*	*0.11*
SEMA4G	**0.35**	0.07	**0.44**	0.13	**0.48**	0.28	**0.89**	0.43	*1.26*	0.61	*0.91*	*0.59*
SEMA5A	**2.38**	0.56	**3.06**	0.45	**3.08**	1.07	**8.98**	7.60	*1.28*	0.61	*0.99*	*0.91*
SEMA5B	**0.45**	0.09	**0.78**	0.18	**2.34**	0.52	**1.32**	0.53	*1.72*	0.17	*0.33*	*0.11*
SEMA6A	**28.24**	6.78	**45.65**	12.14	**12.75**	3.45	**31.24**	4.13	*1.62*	0.26	*3.58*	***0.010***
SEMA6B	**0.73**	0.18	**1.95**	0.78	**9.90**	4.74	**31.22**	30.80	*2.67*	0.07	*0.20*	*0.17*

SEMA6C	**0.05**	0.01	**0.07**	0.03	**0.13**	0.06	**0.06**	0.02	*1.53*	0.28	*0.54*	*0.83*
SEMA6D	**7.30**	1.55	**13.26**	2.93	**4.43**	0.84	**5.70**	1.43	*1.82*	0.11	*3.00*	***0.019***
SEMA7A	**2.85**	0.75	**3.91**	0.35	**0.93**	0.50	**2.99**	1.56	*1.37*	0.48	*4.22*	***0.019***
Chemokines												
CXCL1	**0.18**	0.07	**1.18**	0.32	**4.46**	3.25	**1.30**	1.04	*6.51*	**0.019**	*0.27*	*0.76*
CXCL2	**0.17**	0.08	**0.62**	0.14	**1.10**	0.47	**3.49**	2.96	*3.70*	**0.019**	*0.56*	*0.91*
CXCL8	**0.23**	0.06	**0.51**	0.19	**0.71**	0.15	**0.52**	0.42	*2.22*	0.26	*0.71*	*0.61*
CXCL10	**0.02**	0.01	**0.05**	0.02	**0.04**	0.03	**0.88**	0.47	*1.94**	0.76	*1.09*	*0.66*
CXCL12	**2.51**	0.37	**3.65**	0.70	**30.09**	23.06	**24.58**	16.09	*1.45*	0.35	*0.12*	*0.76*
IL6 family												
CNTF	**0.19**	0.04	**0.52**	0.11	**0.20**	0.11	**0.69**	0.50	*2.66*	**0.019**	*2.65**	*0.069*
CLCF1	**0.02**	0.01	**0.16**	0.13	**0.48**	0.23	**0.55**	0.34	*6.62**	0.35	*0.34*	*0.83*
CTF1	**0.17**	0.03	**0.44**	0.13	**0.82**	0.29	**1.66**	1.36	*2.59*	0.17	*0.54*	*0.61*
IL6	**0.06**	0.02	**0.07**	0.03	**0.38**	0.31	**0.06**	0.02	*1.27*	0.76	*0.19*	*0.83*
IL11	**0.01**	0.00	**0.07**	0.05	**0.04**	0.03	**0.02**	0.01	*5.11**	1.00	*1.63*	*0.91*
LIF	**0.01**	0.00	**0.03**	0.02	**0.76**	0.70	**0.43**	0.37	*5.17**	0.40	*0.04*	*1*
IGFs												
IGF1	**0.35**	0.10	**0.32**	0.12	**0.63**	0.23	**1.46**	0.98	*0.94*	1.00	*0.51*	*0.61*
IGF2	**0.23**	0.01	**0.33**	0.12	**6.04**	4.62	**1.95**	1.23	*1.42*	0.26	*0.06*	*0.39*
Miscellaneous												
CTGF	**1.70**	0.50	**4.53**	0.90	**13.40**	4.85	**9.77**	7.80	*2.67*	**0.038**	*0.34*	*0.26*
FIGF	**0.25**	0.07	**0.28**	0.07	**0.60**	0.51	**0.29**	0.10	*1.09*	0.76	*0.46*	*0.34*
HGF	**0.12**	0.02	**0.37**	0.12	**0.31**	0.14	**0.99**	0.40	*3.05*	0.26	*1.17*	*0.45*
LINGO1	**0.15**	0.11	**0.77**	0.30	**1.42**	0.50	**0.40**	0.14	*5.18*	0.06	*0.54*	*0.61*

CWM: Control white matter, Remyelinated: Remyelinated lesion, Demyelinated: Demyelinated inactive lesion, Active: Demyelinated active lesion, Re/CWM and De/Re ratio: remyelinated vs. control white matter and vs. demyelinated inactive lesions, respectively; p value were calculated by 2-sided U tests, unadjusted for multiple testing. p-values < 0.05 are printed in bold. 0.00: Values were below our detection limit, which was 0.01% *GAPDH*. Specimens analyzed: 6 normal white matter specimens from 4 subjects, 6 demyelinated inactive lesions from 4 subjects, 4 demyelinated active lesions from 3 subjects, and 4 remyelinated lesions from 3 subjects were dissected and used for qPCR analysis. The mean expression values are given as % *GAPDH*; SEM denotes standard error of the mean. * Ratios may be imprecise since at least one value was below or close to the detection limit.

SEMA3C, SEMA4D, SEMA6A, SEMA6D, and SEMA7A were significantly higher expressed in remyelinated lesions as compared to demyelinated lesions. In contrast SEMA4A showed a trend towards higher expression in demyelinated lesions (4.7 fold; $p = 0.067$; Table 2).

LINGO-1 (official gene name *LRRN6A*) is of great current interest, because it is tested as a therapeutic target for MS (EUCTR2011-006262-40-CZ) or First Episode of Acute Optic Neuritis (EUCTR2011-006291-39-SE) [54]. Therefore we provide detailed expression data for this gene in the different types of MS lesions and control tissue although its biology was not further studied here (Additional file 4: Figure S2).

The receptors ERBB3, FGFR2 and MET were significantly higher expressed in re- versus demyelinated lesions (Additional file 3: Table S2). FGFR1, FGFR2, PDGFRB, IL6ST, PLXNB1 and CXCR7 were significantly higher expressed in remyelinated lesions compared to control white matter (Additional file 3: Table S2).

FGF1 is abundant in white matter and further increased in remyelinated lesions

FGF1 was the most abundant FGF both in the white matter of the control brain and in the white matter MS lesions (Figure 1, Table 2). Further, *FGF1* had the highest transcript level of all the analyzed myelination-related factors (Figure 1, Table 2) and was therefore further studied in detail. In remyelinated lesions, *FGF1* showed a trend towards higher expression compared to demyelinated lesions and was significantly higher expressed than in control white matter (Figure 1, Figures 2a,b). We could directly compare *FGF1* expression in two tissue blocks with de- and remyelinated areas within the same lesion: in both blocks *FGF1* transcript levels were higher in the dissected remyelinated areas compared to the demyelinated lesion core (Figures 2 b-e).

Figure 1 Oligodendrocyte regulators are differentially expressed in various lesion types. MS lesions were dissected from frozen tissue and the expression level of the indicated mediators regulating oligodendrocytes were determined by qPCR. The absolute expression levels are given in terms of *% GAPDH*. Displayed is the mean of 6 normal white matter specimens, 6 demyelinated inactive, 4 demyelinated active, and 4 remyelinated lesion areas.

Figure 2 FGF1 expression is elevated in remyelinated lesions. a *FGF1* gene expression was analyzed by quantitative PCR TLDA relative to *GAPDH* in individual lesion areas (Re: remyelinated, De: demyelinated inactive, Active: actively demyelinating areas) and control white matter specimens (Ctrl.). Each symbol represents a single dissected area. Medians (bars) and $1^{st}/3^{rd}$ quartiles (boxes) are shown. Whiskers extend to the range up to 1.5 times of the interquartile range; values beyond were regarded as outliers. We noted one outlier in the six analyzed demyelinated inactive lesions, but we cannot explain why this one lesion had a higher *FGF1* level than all others. Regarding the primary topic of remyelination in this study, we compared the remyelinated lesions with the other groups of tissue specimens; Mann–Whitney U test showed a significant difference between the remyelinated areas and controls ($p < 0.01$), while the differences between remyelinated vs. demyelinated inactive areas ($p = 0.1$) and remyelinated vs. actively demyelinating areas ($p = 0.2$) did not reach statistical significance. **b-d** In two blocks, adjacent de- and remyelinated areas were present within the same lesion and excised for quantitative PCR TLDA analysis (labelled as Block 1 and 2 for Figure 2a-e). *FGF1* expression normalized to *GAPDH* is shown. Fold-changes of *FGF1*

expression between the re- and demyelinated areas in each block were calculated for the different housekeeping genes. The geometric mean of these fold changes obtained by normalization to the three housekeeping genes was 2.1× for block 1 and 4.1× for block 2.

Accordingly, FGF1 staining was more prominent in the re- compared to the demyelinated lesion area (Figures 3 a-c). Analyzing control brain for FGF1 expression, we found cortical neurons to be FGF1 positive (Figure 3 d). Furthermore, FGF1 staining was detected in cells which, according to their morphology, could be oligodendroglia (Figures 3 e-f). These FGF1-positive oligodendroglia could also be detected in NAWM of MS brain (data not shown). Double staining of FGF1 and GFAP revealed astrocytes in remyelinated lesions to be FGF1 positive (Figure 4a). In contrast, reactive astrocytes detected in NAWM surrounding the lesion areas were FGF1 negative (Figure 4b). In active lesions we detected subsets of microglia/macrophages to be FGF1 positive (Figure 4c). Furthermore, subsets of B and T cells present in perivascular cuffs displayed an FGF1 staining (Figures 4d, e). Together, our stainings localized FGF1 to astrocytes, oligodendrocytes, microglia/macrophages and infiltrating lymphocytes, but we cannot conclude from our stainings which cells are the major sources and why it is produced.

Figure 3 FGF1 is expressed in re- and demyelinated lesions as well as in neurons and oligodendroglia in control brain and NAWM. a LFB staining of an MS tissue specimen with demyelinated (De), remyelinated (Re) lesion areas along with normal appearing white mater (NAWM) and gray matter (GM). The FGF staining was more prominent in the remyelinated area **b** compared to the chronic inactive demyelinated area **c**. In control brain, FGF1 staining was detected in neurons of gray matter **d** and cells appearing as oligodendrocytes in WM **e, f**. Scale bars: 20 μm

Figure 4 FGF1 is displayed by astrocytes, microglia/macrophages and lymphocytes. Double immunofluorescence staining of FGF1 with GFAP **a, b**, Iba-1 **c**, CD3 **d**, and CD20 **e**. Pictures were taken from different areas, namely a chronic inactive demyelinated lesion **a**, NAWM **b**, chronic active lesion **c**, and perivascular cuffs in an active lesion **d, e**. Scale bars: a and b 12.5 μm; **c**, **d** and **e** 25 μm.

FGF1 accelerates developmental myelination in dissociated cultures

FGF1 was the most abundant of all the myelination-related mediators included in this study (Table 2) and was further up-regulated in remyelinated lesions. This led us to speculate that increased availability of this member of the FGF family supported lesion repair. The validity of this concept was first explored in myelinating cultures derived from embryonic rat spinal cord in which myelination is initiated after 12 days *in vitro* and reaches a plateau two weeks later [42,44].

Three independent conditions were used to assess ability of FGF1 to stimulate myelination in these cultures. First, FGF1 was added for four days after the onset of myelination and this enhanced myelination up to 1.7 fold ($p < 0.0001$) (Figures 5a and 5b). Second, FGF1 was added before the onset of myelination at day 12 for a total of 16 days. Again, we observed FGF1 enhanced myelination, particularly at 18 and 24 days in vitro (DIV) (Figure 5c). Third, FGF1 was added before the onset of myelination for 6 days (12–18 DIV) and then withdrawn while myelination was still ongoing. Enhanced myelination could already be detected during the initial phase of myelination, was still seen six days after FGF1 was withdrawn and then

disappeared thereafter (Figure 5d). This indicates that FGF1 accelerates myelination in this culture system.

Figure 5 FGF1 promotes myelination in dissociated spinal cord cultures. Myelinating cultures were treated with different concentrations of FGF1 from 22 DIV to 26 DIV and then stained for myelin (MBP in green) and axons (SMI-31 in red). **a** FGF1 treated cultures showed enhanced levels of MBP^+ myelin sheath as compared to the control cultures. Magnification: left panel = 10X, right panel = 40X. **b** Quantitative evaluation:FG1 promotes myelination ****P <0.0001. Error bars represent SEM of two experiments. Myelinating cultures were treated with 100 ng/ml FGF1 for different time periods. Axonal density calculated as pixel for NFL (different FGF1 dosages/control) were 1.17 for 5 ng/ml FGF1, 1.2 for 50 ng/ml FGF1 and 1.06 for 50 ng/ml FGF1. **c** 16 days (12 DIV to 28 DIV) and **d** 6 days (12 DIV to 18 DIV). The myelination was enhanced at day 18 and 24, but unaltered at day 28. ****P <0.0001. Significance of data values was analyzed using T-test. Error bars represent SEM from three independent experiments. The axonal densities (FGF1/control) ranged between 0.98 and 1.02 in the experiments shown in **c** and **d**.

FGF1 promotes remyelination in cerebellar slice cultures

To determine whether FGF1 would also promote remyelination, we investigated its effects on demyelinated organotypic cerebellar cultures derived from newborn mouse pups. Slice cultures myelinated *in vitro* in 12 days, they were then demyelinated using lysolecithin and allowed to recover in the presence or absence of FGF1. Analysis of cultures 14 days later revealed FGF1 promoted remyelination as assessed by immunofluorescence microscopy that identified approximately 1.5 fold increase in myelin basic protein (MBP) immunoreactivity (Figures 6a and 6b). The MBP expression was normalized based on the axonal density as measured by NFL staining. This increase in MBP positive immunoreactivity was paralleled by an increase of *Mbp* transcripts (Figure 6c). Further, we observed an increase in transcript level of *Mag* (Figure 6d), but not consistently of *Mog* (Figure 6e).

Figure 6 FGF1 enhances remyelination in organotypic cerebellar slice cultures. After toxic demyelination, cerebellar slice cultures were allowed to remyelinate for 14 days in the absence or presence of 100 ng/ml FGF1. Myelination was assessed by immunostaining **(a, b)** and quantitative PCR **(c–e). a** MBP (red), NFL (green) scale bar = 50 μm **b** Quantification of MBP^+/NFL^+ area ratio in FGF1 treated slices compared to untreated controls. MBP^+ myelin formation is promoted by FGF1. Students t-test *P = 0.0341. **c-e** After 14 days RNA was extracted, cDNA obtained and transcript levels of **c** MBP, **d** *Mag* and **e** *Mog* were measured by qPCR. One-way ANOVA **P < 0.01; *P < 0.05; All error bars represent SEM from three independent experiments.

FGF1 decelerates differentiation of monocultured OPCs

To determine the effect of FGF1 on the proliferation of monocultured oligodendroglial cells we cultured OPCs in the presence of PDGF-AA, NT3 and different concentrations of FGF1 for 24 or 48 hours. No significant influence on the proliferation capacity of OPCs after 24 and 48 hours compared to controls could be shown by BrdU assays (Figure 7a). To analyse effects of FGF1 on oligodendroglial differentiation, different concentrations of FGF1 were added to differentiating oligodendrocytes for up to 48 hours. The differentiation of oligodendrocytes was analyzed using morphological parameters as well as the mRNA expression levels of several genes coding for myelin proteins. Addition of FGF1 for 48 h

decreased significantly the number of mature oligodendrocytes characterized by multiple processes and complex branching (Figure 7b). To further examine the effect on oligodendroglial differentiation we analyzed the mRNA expression levels of myelin proteins *(Mbp, Mag,* and *Mog)* at different time points. The expression levels of all genes were significantly down regulated after exposure to FGF1 (Figures 7 c-e).

Figure 7 FGF1 decelerates differentiation of monocultured oligodendrocytes. a FGF1 does not affect proliferation of primary murine OPCs but **b** decelerates the differentiation into myelinating oligodendrocytes as determined by morphology; Two-way ANOVA with Bonferroni post correction **p < 0.01; *p < 0.05. The expression of myelin-associated genes was assessed by quantitative RT-PCR on samples from OPCs (6 h), immature (24 h) and mature cells (48 h). The expression levels of **c** *Mbp*, **d** *Mag* and in **e** *Mog* are reduced due to increasing FGF1 concentrations; one-way ANOVA with Bonferroni post correction *** p < 0.001 **P < 0.01; *P = <0.05; error bars represent SEM from three independent experiments.

FGF1 induces transcriptional changes in human astrocytes including upregulation of *CXCL8* and *LIF*

Since *FGF1* is highly abundant in MS lesions (Figure 1) and astrocytes are known to express FGFRs [55,56], we analyzed transcriptional responses of human astrocytes to FGF1. First, we established the response of our cultured human astrocytes to FGF1 by analyzing the induction of *HMOX1*, which has been reported to be induced in rodent astrocytes by FGF1 [56]. The interaction of FGF1 with its receptors is stabilized and stimulation efficacy is increased by binding to heparan sulfate [57-60]. Experiments to establish appropriate stimulation conditions showed that 5 U/ml heparin and 10 ng/ml FGF1 caused a reliable up-regulation of *HMOX1*, while heparin alone had no effect on (Figure 8 and data not shown).

Figure 8 FGF1-induced gene expression in human primary astrocytes. (a-c) Gene expression was analysed after 8 h **(a)** and 24 h **(b)** h with and without FGF1 (10 ng/ml). In all experiments, FGF1 was applied together with heparin (5 U/ml); control cultures contained heparin only. Only differentially expressed probes (corrected p-value <0.05, fold change > 1.4-fold up or down, and normalized mean expression intensity ≥ 100 in any one of the two groups) are shown. The number of differentially expressed probes is shown in **a**. *CXCL8* and *LIF* were among the genes upregulated at both time points (see also Additional file 5: Table S3). **(d)** For validation, *CXCL8*, *LIF*, and the positive control *HMOX1* gene expression were analysed by quantitative PCR after 8 h and 24 h with FGF1 (10 ng/ml). **(e)** Secreted CXCL-8 and LIF protein were measured by ELISA in the supernatant after 8 and 24 h with and without 10 ng/ml FGF1. In **(d,e)**, the fold-change compared to unstimulated control cultures is displayed. Black bars and boxes indicate medians and $1^{st}/3^{rd}$ quartiles, respectively. Whiskers extend to the most extreme samples up to 1.5× of the IQR. Red bars indicate means. Fold-changes were analysed by two-sided one-sample tests against the control samples ($\mu = 1$; t-test for FGF1 mRNA, U test for FGF1 protein because of non-normal distribution). *: $p < 0.05$, **: $p < 0.01$.

Further, the effects of FGF1 stimulation on primary human astrocytes were investigated using an Affymetrix GeneChip® Human Gene 1.0 ST Array. Triplicate samples were analyzed at 8 h and 24 h. Differential expression analysis between FGF-treated astrocytes and control cultures identified 292 probe sets (154 upregulated and 138 downregulated) at 8 h and 933 probe sets (521 upregulated and 412 downregulated) at 24 h (Figures 8a-c). Accordingly, unsupervised hierarchical clustering based on the transcriptional signatures at 8 and 24 h

clustered together the FGF1 replicates and classified them apart from the control replicates (heatmaps in Figures 8b,c). Interestingly, 245 out of 292 (about 85%) of differentially expressed probe sets at 8 h maintained differential expression at 24 h. All probe sets regulated by FGF1 at 8 and 24 h and the genes they represent are shown in Additional file 5: Table S3. Among these genes regulated by FGF1 were two released factors that had been linked previously to remyelination, namely *LIF* and *CXCL8*. We then validated the induction of *CXCL8* and *LIF* in human astrocytes by FGF1 further by both qPCR and ELISA (Figures 8d,e).

Discussion

This study presents a quantitative expression analysis of remyelinated MS lesions. We describe a complex change of multiple factors known to affect oligodendrocyte proliferation and maturation. Among all 46 analyzed factors, *FGF1* was the most abundant one in shadow plaques and was further induced in these lesions. In functional experiments with dissociated myelinating cultures and remyelinating slice cultures, we found that FGF1 promotes both developmental myelination and remyelination.

FGF family members are widely expressed in the brain, and are recognized as determinants of neuronal survival during development and adulthood [61]. Here we identified a role for FGF1 in promoting remyelination with potential relevance for repair in human MS. This is consistent with previous findings showing a role of the FGF family in myelination [39,62,63].

In MS lesions, FGF1 was localized on astrocytes, neurons, oligodendrocytes, microglia and infiltrating T cells and B cells. Previously FGF1 was reported in neurons [64] and reactive astrocytes in Alzheimer's disease [65]. In an animal model of chemically induced demyelination, enhanced expression of FGF1 was described during remyelination [66]. Our qPCR analysis indicated a higher level of *FGF1* also in active lesions. In addition, our immunostaining localized FGF1 on T cells and microglia in active MS lesions. FGF1 could be produced by these cells themselves or alternatively been picked up after release from surrounding cells. Our qPCR shows that in normal brain and in the different MS lesions, *FGF1* is abundantly transcribed, but the precise stimuli triggering FGF1 expression during experimental de- and remyelination and in remyelinated MS lesions remain to be identified.

MS lesions frequently show a demyelinated core and a remyelinating ring [11]. Examining two such tissue blocks we found *FGF1* to be higher in the remyelinated rim compared to the demyelinated core. This further indicates that success of remyelination is associated with increased levels of FGF1. The up-regulation of *FGF1* was found in remyelinated areas, in which the repair had already been carried out before. Therefore our tissue analysis would not allow concluding whether FGF1 is involved in active remyelination and/or maintenance of remyelinated myelin sheaths. Our functional experiments, however, indicate that FGF1 has a role in the active myelination and remyelination process. In an *in vitro* culture system recapitulating essential features of myelination [42-44] we found FGF1 to promote developmental myelination. The significance of the FGF family in developmental myelination has been established *in vivo*: Fibroblast growth factor receptor (FGFR) signaling is required for the generation of OPCs from the embryonic forebrain [63]. Remyelination and developmental myelination share essential features, but possible differences between development and repair have to be considered [67]. Therefore, we employed a slice culture model [45,48] and found that FGF1 promoted also remyelination.

Our further experiments with pure cultures of oligodendrocytes and astrocytes suggest that the (re)myelination promoting effect of FGF1 is mediated by an indirect mechanism: FGF1 promoted (re)myelination in mixed cultures and slice cultures that contained oligodendrocytes, microglia, and astrocytes. In pure oligodendrocyte cultures, however, FGF1 did not induce proliferation and inhibited the differentiation. Therefore we analyzed if FGF1 might induce myelination-promoting factors in astrocytes. We switched for these experiments to human astrocytes, since understanding of regulation of remyelination in MS is our purpose. We found that FGF1 induced LIF and CXCL8 in primary human astrocytes. CXCL8, which does not have a homologue in rats and mice, is not only a chemoattractant for monocytes and neutrophils, but also recruits oligodendrocyte progenitor cells [68]. CXCL8 was detected in astrocytes around active MS lesions [69]; its receptors CXCR2 and CXCR1 [70] were found on oligodendrocyte precursor cells [71] and, importantly, upregulated on oligodendrocytes around MS lesions [68]. CXCL8 was therefore suggested to be involved in regeneration of MS lesions [69]. LIF has been established to support oligodendrocyte survival *in vitro* [72,73] and *in vivo* [74,75] as well as to promote myelination [76]. In EAE models, LIF directly prevented oligodendrocyte cell death [74] and promoted remyelination [77]. Together, we found that human astrocytes produce CXCL8 and LIF in response to FGF1, and these findings together with our results obtained with rodent culture systems (myelinating dissociated cultures, remyelinating slice cultures, and pure oligodendrocytes) indicate that FGF1 promotes the induction of (re)myelination indirectly via an effect mediated by astrocytes, although the relative importance of different FGF1-induced factors in the rodent models of remyelination remains to be specified. One constant feature of remyelination is that the repaired myelin is thinner than the original myelin [78], but it is unclear why this is the case. Previous findings that FGFR signaling regulates myelin thickness in development [39] raise the possibility that FGFs may participate in the regulation of this aspect of remyelination.

Beyond the FGF-family, our study provides quantitative information on additional regulators of oligodendrocytes biology in de- and remyelinated human MS lesions such as Lingo-1, which is a target in current clinical trials [27,54]. Semaphorins were originally identified as axonal guidance cues, but they also regulate migration and oligodendrocyte biology [29,31,79]. We noted that 5 semaphorins (*3C, 4D, 6A, 6D,* and *7A*) were significantly higher expressed in re- versus demyelinated lesions. *Sema6A* and *Sema6D* had not been linked before to remyelination in MS. All this inspires further studies on the role of semaphorins in the regulation of remyelination in MS.

Mediators commonly used to promote oligodendrocyte cultures such as FGF2, PDGF, ciliary neurotrophic factor (CNTF), IGFs, and IL-11 were present or even enhanced in inactive demyelinated MS lesions. This adds to the view that it is not the scarcity or even lack of one specific factor in the inactive demyelinated lesions that can explain the failure of remyelination. Since myelination depends on a delicate and fine-tuned balance of many factors [78], the multiple alterations observed here (Table 1) may well contribute to the failure of remyelination together with the induction of inhibitory mechanisms.

In summary, we present a quantitative analysis of oligodendrocyte regulators in remyelinated MS lesions. We report that success of remyelination in MS is accompanied by high levels of *FGF1* and that FGF1 enhances myelination and remyelination *in vitro* presumably via an indirect mechanism mediated by astrocytes. Targeting FGF family members may have therapeutic potential [80], and should be tested to enhance repair in MS.

Abbreviations

ABI, Applied Biosystems; BAFF, B cell activating factor of the TNF family; CNTF, Ciliary neurotrophic factor; DAB, Diaminobenzidine; DIV, Day *in vitro*; FFPE, Formalin fixed paraffin embeded; FGF, Fibroblast growth factor; FGFR, Fibroblast growth factor receptor; GFAP, Glial fibrillary acidic protein; hARP, Human acid ribosomal protein; IGF, Insulin derived growth factor; LDA, Low density array; LIF, Leukemia inhibitory factor; LFB, Luxol fast blue; MAG, Myelin associated glycoprotein; MBP, Myelin basic protein; MOG, Myelin oligodendrocyte glycoprotein; MS, Multiple sclerosis; OPCs, Oligodendrocyte progenitor cells; P0, Newborn; PAP, Peroxidase anti peroxidase; PDGF, Platelet derived growth factor; PPIA, Peptidylprolyl isomerase A; qPCR, Quantitative PCR; RT, Room temperature.

Competing interests

The authors declare that they have no competing interests.

Acknowledgements

We thank the Netherlands Brain Bank, the UK MS Brain Bank, the NeuroResource tissue bank, UCL London for tissue samples. We are grateful to Dr. F. Aloisi, Rome, for providing us with primary human astrocytes. We thank Drs. K. Dornmair and N. Kawakami for comments on the manuscript. This study was supported by the Deutsche Forschungsgemeinschaft (SFB-TR 128) and SyNergy, the Klinisches Kompetenznetz Multiple Sklerose and the Verein zur Therapieforschung für MS Kranke, the Interdisciplinary Center for Clinical Research (IZKF) (KuT3/006/11 to TK), and Fondazione Italiana Sclerosi Multipla (2012/R/7 to CF).

References

1. Tripathi RB, Rivers LE, Young KM, Jamen F, Richardson WD (2010) NG2 glia generate new oligodendrocytes but few astrocytes in a murine experimental autoimmune encephalomyelitis model of demyelinating disease. J Neurosci 30(48):16383–16390, doi: 10.1523/jneurosci. 3411-10.2010

2. Franklin RJ (2002) Why does remyelination fail in multiple sclerosis? Nature Rev Neurosci 3(9):705–714

3. Piaton G, Williams A, Seilhean D, Lubetzki C (2009) Remyelination in multiple sclerosis. Prog Brain Res 175:453–464, doi: 10.1016/s0079-6123(09)17530-1

4. Redford EJ, Kapoor R, Smith KJ (1997) Nitric oxide donors reversibly block axonal conduction: demyelinated axons are especially susceptible. Brain 120(Pt 12):2149–2157

5. Nave KA, Trapp BD (2008) Axon-glial signaling and the glial support of axon function. Annu Rev Neurosci 31:535–561

6. Funfschilling U, Supplie LM, Mahad D, Boretius S, Saab AS, Edgar J, Brinkmann BG, Kassmann CM, Tzvetanova ID, Mobius W, Diaz F, Meijer D, Suter U, Hamprecht B, Sereda MW, Moraes CT, Frahm J, Goebbels S, Nave KA (2012) Glycolytic oligodendrocytes maintain myelin and long-term axonal integrity. Nature 485(7399):517–521, doi: 10.1038/nature11007

7. Lee Y, Morrison BM, Li Y, Lengacher S, Farah MH, Hoffman PN, Liu Y, Tsingalia A, Jin L, Zhang PW, Pellerin L, Magistretti PJ, Rothstein JD (2012) Oligodendroglia metabolically support axons and contribute to neurodegeneration. Nature 487(7408):443–448, doi: 10.1038/nature11314

8. Patani R, Balaratnam M, Vora A, Reynolds R (2007) Remyelination can be extensive in multiple sclerosis despite a long disease course. Neuropathol Appl Neurobiol 33(3):277–287, doi: 10.1111/j.1365-2990.2007.00805.x

9. Patrikios P, Stadelmann C, Kutzelnigg A, Rauschka H, Schmidbauer M, Laursen H, Sorensen PS, Bruck W, Lucchinetti C, Lassmann H (2006) Remyelination is extensive in a subset of multiple sclerosis patients. Brain 129(Pt 12):3165–3172

10. Prineas JW, Barnard RO, Kwon EE, Sharer LR, Cho ES (1993) Multiple sclerosis: remyelination of nascent lesions. Ann Neurol 33(2):137–151, doi: 10.1002/ana.410330203

11. Prineas JW, Connell F (1979) Remyelination in multiple sclerosis. Ann Neurol 5(1):22–31, doi: 10.1002/ana.410050105

12. Raine CS, Wu E (1993) Multiple sclerosis: remyelination in acute lesions. J Neuropathol Exp Neurol 52(3):199–204

13. Chang A, Tourtellotte WW, Rudick R, Trapp BD (2002) Premyelinating oligodendrocytes in chronic lesions of multiple sclerosis. NEnglJMed 346(3):165–173

14. Chang A, Staugaitis SM, Dutta R, Batt CE, Easley KE, Chomyk AM, Yong VW, Fox RJ, Kidd GJ, Trapp BD (2012) Cortical remyelination: a new target for repair therapies in multiple sclerosis. Ann Neurol 72(6):918–926, doi: 10.1002/ana.23693

15. Franklin RJ, Ffrench-Constant C (2008) Remyelination in the CNS: from biology to therapy. Nature Rev Neurosci 9(11):839–855

16. Kotter MR, Stadelmann C, Hartung HP (2011) Enhancing remyelination in disease–can we wrap it up? Brain 134(Pt 7):1882–1900, doi: 10.1093/brain/awr014

17. Kremer D, Aktas O, Hartung HP, Kury P (2011) The complex world of oligodendroglial differentiation inhibitors. Ann Neurol 69(4):602–618

18. Ransohoff RM, Cardona AE (2010) The myeloid cells of the central nervous system parenchyma. Nature 468(7321):253–262, doi: 10.1038/nature09615

19. Williams A, Piaton G, Lubetzki C (2007) Astrocytes–friends or foes in multiple sclerosis? Glia 55(13):1300–1312, doi: 10.1002/glia.20546

20. Back SA, Tuohy TM, Chen H, Wallingford N, Craig A, Struve J, Luo NL, Banine F, Liu Y, Chang A, Trapp BD, Bebo BF Jr, Rao MS, Sherman LS (2005) Hyaluronan accumulates in demyelinated lesions and inhibits oligodendrocyte progenitor maturation. Nat Med 11(9):966–972

21. Charles P, Hernandez MP, Stankoff B, Aigrot MS, Colin C, Rougon G, Zalc B, Lubetzki C (2000) Negative regulation of central nervous system myelination by polysialylated-neural cell adhesion molecule. Proc Natl Acad Sci U S A 97(13):7585–7590, doi: 10.1073/pnas.100076197

22. Charles P, Reynolds R, Seilhean D, Rougon G, Aigrot MS, Niezgoda A, Zalc B, Lubetzki C (2002) Re-expression of PSA-NCAM by demyelinated axons: an inhibitor of remyelination in multiple sclerosis? Brain 125(Pt 9):1972–1979

23. Czopka T, Holst A, Ffrench-Constant C, Faissner A (2010) Regulatory mechanisms that mediate tenascin C-dependent inhibition of oligodendrocyte precursor differentiation. J Neurosci 30(37):12310–12322

24. John GR, Shankar SL, Shafit-Zagardo B, Massimi A, Lee SC, Raine CS, Brosnan CF (2002) Multiple sclerosis: re-expression of a developmental pathway that restricts oligodendrocyte maturation. Nat Med 8(10):1115–1121

25. Kremer D, Heinen A, Jadasz J, Gottle P, Zimmermann K, Zickler P, Jander S, Hartung HP, Kury P (2009) p57kip2 is dynamically regulated in experimental autoimmune encephalomyelitis and interferes with oligodendroglial maturation. Proc Natl Acad Sci U S A 106(22):9087–9092

26. Lau LW, Keough MB, Haylock-Jacobs S, Cua R, Doring A, Sloka S, Stirling DP, Rivest S, Yong VW (2012) Chondroitin sulfate proteoglycans in demyelinated lesions impair remyelination. Ann Neurol 72(3):419–432, doi: 10.1002/ana.23599

27. Mi S, Miller RH, Lee X, Scott ML, Shulag-Morskaya S, Shao Z, Chang J, Thill G, Levesque M, Zhang M, Hession C, Sah D, Trapp B, He Z, Jung V, McCoy JM, Pepinsky RB (2005) LINGO-1 negatively regulates myelination by oligodendrocytes. Nat Neurosci 8(6):745–751, doi: 10.1038/nn1460

28. Mohan H, Krumbholz M, Sharma R, Eisele S, Junker A, Sixt M, Newcombe J, Wekerle H, Hohlfeld R, Lassmann H, Meinl E (2010) Extracellular matrix in multiple sclerosis lesions: fibrillar collagens, biglycan and decorin are upregulated and associated with infiltrating immune cells. Brain Pathol 20(5):966–975

29. Piaton G, Aigrot MS, Williams A, Moyon S, Tepavcevic V, Moutkine I, Gras J, Matho KS, Schmitt A, Soellner H, Huber AB, Ravassard P, Lubetzki C (2011) Class 3 semaphorins influence oligodendrocyte precursor recruitment and remyelination in adult central nervous system. Brain 134(Pt 4):1156–1167, doi: 10.1093/brain/awr022

30. Preston M, Gong X, Su W, Matsumoto SG, Banine F, Winkler C, Foster S, Xing R, Struve J, Dean J, Baggenstoss B, Weigel PH, Montine TJ, Back SA, Sherman LS (2013) Digestion products of the PH20 hyaluronidase inhibit remyelination. Ann Neurol 73(2):266–280, doi: 10.1002/ana.23788

31. Williams A, Piaton G, Aigrot MS, Belhadi A, Theaudin M, Petermann F, Thomas JL, Zalc B, Lubetzki C (2007) Semaphorin 3A and 3 F: key players in myelin repair in multiple sclerosis? Brain 130(Pt 10):2554–2565, doi: 10.1093/brain/awm202

32. Yuen TJ, Johnson KR, Miron VE, Zhao C, Quandt J, Harrisingh MC, Swire M, Williams A, McFarland HF, Franklin RJ, Ffrench-Constant C (2013) Identification of endothelin 2 as an inflammatory factor that promotes central nervous system remyelination. Brain 136(Pt 4):1035–1047, doi: 10.1093/brain/awt024

33. Dutta R, Trapp BD (2012) Gene expression profiling in multiple sclerosis brain. Neurobiol Dis 45(1):108–114, doi: 10.1016/j.nbd.2010.12.003

34. Steinman L, Zamvil S (2003) Transcriptional analysis of targets in multiple sclerosis. Nat Rev Immunol 3(6):483–492

35. Zeis T, Graumann U, Reynolds R, Schaeren-Wiemers N (2008) Normal-appearing white matter in multiple sclerosis is in a subtle balance between inflammation and neuroprotection. Brain 131(Pt 1):288–303, doi: 10.1093/brain/awm291

36. Bansal R, Pfeiffer SE (1997) Regulation of oligodendrocyte differentiation by fibroblast growth factors. Adv Exp Med Biol 429:69–77

37. Cohen RI, Chandross KJ (2000) Fibroblast growth factor-9 modulates the expression of myelin related proteins and multiple fibroblast growth factor receptors in developing oligodendrocytes. J Neurosci Res 61(3):273–287

38. Fortin D, Rom E, Sun H, Yayon A, Bansal R (2005) Distinct fibroblast growth factor (FGF)/FGF receptor signaling pairs initiate diverse cellular responses in the oligodendrocyte lineage. J Neurosci 25(32):7470–7479

39. Furusho M, Dupree JL, Nave KA, Bansal R (2012) Fibroblast growth factor receptor signaling in oligodendrocytes regulates myelin sheath thickness. J Neurosci 32(19):6631–6641, doi: 10.1523/jneurosci. 6005-11.2012

40. Zhou YX, Pannu R, Le TQ, Armstrong RC (2012) Fibroblast growth factor 1 (FGFR1) modulation regulates repair capacity of oligodendrocyte progenitor cells following chronic demyelination. Neurobiol Dis 45(1):196–205, doi: 10.1016/j.nbd.2011.08.004

41. Engele J, Bohn MC (1992) Effects of acidic and basic fibroblast growth factors (aFGF, bFGF) on glial precursor cell proliferation: age dependency and brain region specificity. Dev Biol 152(2):363–372

42. Elliott C, Lindner M, Arthur A, Brennan K, Jarius S, Hussey J, Chan A, Stroet A, Olsson T, Willison H, Barnett SC, Meinl E, Linington C (2012) Functional identification of pathogenic autoantibody responses in patients with multiple sclerosis. Brain 135(Pt 6):1819–1833, doi: 10.1093/brain/aws105

43. Sorensen A, Alekseeva T, Katechia K, Robertson M, Riehle MO, Barnett SC (2007) Long-term neurite orientation on astrocyte monolayers aligned by microtopography. Biomaterials 28(36):5498–5508, doi: 10.1016/j.biomaterials.2007.08.034

44. Thomson CE, Hunter AM, Griffiths IR, Edgar JM, McCulloch MC (2006) Murine spinal cord explants: a model for evaluating axonal growth and myelination in vitro. J Neurosci Res 84(8):1703–1715, doi: 10.1002/jnr.21084

45. Birgbauer E, Rao TS, Webb M (2004) Lysolecithin induces demyelination in vitro in a cerebellar slice culture system. J Neurosci Res 78(2):157–166, doi: 10.1002/jnr.20248

46. Miron VE, Jung CG, Kim HJ, Kennedy TE, Soliven B, Antel JP (2008) FTY720 modulates human oligodendrocyte progenitor process extension and survival. Ann Neurol 63(1):61–71

47. Eisele S, Krumbholz M, Fischer MT, Mohan H, Junker A, Arzberger T, Hohlfeld R, Bradl M, Lassmann H, Meinl E (2012) Prospects of transcript profiling for mRNAs and microRNAs using formalin fixed and paraffin embedded dissected autoptic multiple sclerosis lesions. Brain Pathol 22(5):607–618

48. Miron VE, Ludwin SK, Darlington PJ, Jarjour AA, Soliven B, Kennedy TE, Antel JP (2010) Fingolimod (FTY720) enhances remyelination following demyelination of organotypic cerebellar slices. Am J Pathol 176(6):2682–2694

49. Watkins TA, Emery B, Mulinyawe S, Barres BA (2008) Distinct stages of myelination regulated by gamma-secretase and astrocytes in a rapidly myelinating CNS coculture system. Neuron 60(4):555–569, doi: 10.1016/j.neuron.2008.09.011

50. Aloisi F, Borsellino G, Samoggia P, Testa U, Chelucci C, Russo G, Peschle C, Levi G (1992) Astrocyte cultures from human embryonic brain: characterization and modulation of surface molecules by inflammatory cytokines. J Neurosci Res 32(4):494–506

51. Krumbholz M, Theil D, Derfuss T, Rosenwald A, Schrader F, Monoranu CM, Kalled SL, Hess DM, Serafini B, Aloisi F, Wekerle H, Hohlfeld R, Meinl E (2005) BAFF is produced by astrocytes and up-regulated in multiple sclerosis lesions and primary central nervous system lymphoma. J Exp Med 201(2):195–200

52. Irizarry RA, Hobbs B, Collin F, Beazer-Barclay YD, Antonellis KJ, Scherf U, Speed TP (2003) Exploration, normalization, and summaries of high density oligonucleotide array probe level data. Biostatistics 4(2):249–264, doi: 10.1093/biostatistics/4.2.249

53. Smyth GK (2004) Linear models and empirical bayes methods for assessing differential expression in microarray experiments. Stat Appl Genet Mol Biol 3:Article3, doi:10.2202/1544-6115.1027

54. Rudick RA, Mi S, Sandrock AW Jr (2008) LINGO-1 antagonists as therapy for multiple sclerosis: in vitro and in vivo evidence. Expert Opin Biol Ther 8(10):1561–1570, doi: 10.1517/14712598.8.10.1561

55. Takami K, Matsuo A, Terai K, Walker DG, McGeer EG, McGeer PL (1998) Fibroblast growth factor receptor-1 expression in the cortex and hippocampus in Alzheimer’s disease. Brain Res 802(1–2):89–97

56. Vargas MR, Pehar M, Cassina P, Martinez-Palma L, Thompson JA, Beckman JS, Barbeito L (2005) Fibroblast growth factor-1 induces heme oxygenase-1 via nuclear factor erythroid 2-related factor 2 (Nrf2) in spinal cord astrocytes: consequences for motor neuron survival. J Biol Chem 280(27):25571–25579, doi: 10.1074/jbc.M501920200

57. Yayon A, Klagsbrun M, Esko JD, Leder P, Ornitz DM (1991) Cell surface, heparin-like molecules are required for binding of basic fibroblast growth factor to its high affinity receptor. Cell 64(4):841–848

58. Gospodarowicz D, Cheng J (1986) Heparin protects basic and acidic FGF from inactivation. J Cell Physiol 128(3):475–484, doi: 10.1002/jcp.1041280317

59. Spivak-Kroizman T, Lemmon MA, Dikic I, Ladbury JE, Pinchasi D, Huang J, Jaye M, Crumley G, Schlessinger J, Lax I (1994) Heparin-induced oligomerization of FGF molecules is responsible for FGF receptor dimerization, activation, and cell proliferation. Cell 79(6):1015–1024, doi:http://dx.doi.org/10.1016/0092-8674(94)90032-9

60. Shao N, Wang H, Zhou T, Xue Y, Liu C (1994) Heparin potentiation of the effect of acidic fibroblast growth factor on astrocytes and neurons. Life Sci 54(12):785–789, doi:http://dx.doi.org/10.1016/0024-3205(94)00447-1

61. Reuss B, von Bohlen und Halbach O (2003) Fibroblast growth factors and their receptors in the central nervous system. Cell Tissue Res 313(2):139–157, doi: 10.1007/s00441-003-0756-7

62. Besnard F, Perraud F, Sensenbrenner M, Labourdette G (1989) Effects of acidic and basic fibroblast growth factors on proliferation and maturation of cultured rat oligodendrocytes. Int J Dev Neurosci 7(4):401–409

63. Furusho M, Kaga Y, Ishii A, Hebert JM, Bansal R (2011) Fibroblast growth factor signaling is required for the generation of oligodendrocyte progenitors from the embryonic forebrain. J Neurosci 31(13):5055–5066, doi: 10.1523/jneurosci. 4800-10.2011

64. Elde R, Cao YH, Cintra A, Brelje TC, Pelto-Huikko M, Junttila T, Fuxe K, Pettersson RF, Hokfelt T (1991) Prominent expression of acidic fibroblast growth factor in motor and sensory neurons. Neuron 7(3):349–364

65. Kimura H, Tooyama I, McGeer PL (1994) Acidic FGF expression in the surroundings of senile plaques. Tohoku J Exp Med 174(3):279–293

66. Tourbah A, Baron-Van Evercooren A, Oliver L, Raulais D, Jeanny JC, Gumpel M (1992) Endogenous aFGF expression and cellular changes after a demyelinating lesion in the spinal cord of adult normal mice: immunohistochemical study. J Neurosci Res 33(1):47–59, doi: 10.1002/jnr.490330107

67. Fancy SP, Harrington EP, Yuen TJ, Silbereis JC, Zhao C, Baranzini SE, Bruce CC, Otero JJ, Huang EJ, Nusse R, Franklin RJ, Rowitch DH (2011) Axin2 as regulatory and therapeutic target in newborn brain injury and remyelination. Nat Neurosci 14(8):1009–1016, doi: 10.1038/nn.2855

68. Kelland EE, Gilmore W, Weiner LP, Lund BT (2011) The dual role of CXCL8 in human CNS stem cell function: multipotent neural stem cell death and oligodendrocyte progenitor cell chemotaxis. Glia 59(12):1864–1878, doi: 10.1002/glia.21230

69. Omari KM, John GR, Sealfon SC, Raine CS (2005) CXC chemokine receptors on human oligodendrocytes: implications for multiple sclerosis. Brain 128(Pt 5):1003–1015

70. Semple BD, Kossmann T, Morganti-Kossmann MC (2010) Role of chemokines in CNS health and pathology: a focus on the CCL2/CCR2 and CXCL8/CXCR2 networks. J Cereb Blood Flow Metable 30(3):459–473, doi: 10.1038/jcbfm.2009.240

71. Nguyen D, Stangel M (2001) Expression of the chemokine receptors CXCR1 and CXCR2 in rat oligodendroglial cells. Dev Brain Res 128(1):77–81, doi:http://dx.doi.org/10. 1016/S0165-3806(01)00128-6

72. Mayer M, Bhakoo K, Noble M (1994) Ciliary neurotrophic factor and leukemia inhibitory factor promote the generation, maturation and survival of oligodendrocytes in vitro. Development 120(1):143–153

73. Barres BA, Schmid R, Sendnter M, Raff MC (1993) Multiple extracellular signals are required for long-term oligodendrocyte survival. Development 118(1):283–295

74. Butzkueven H, Zhang J-G, Soilu-Hanninen M, Hochrein H, Chionh F, Shipham KA, Emery B, Turnley AM, Petratos S, Ernst M, Bartlett PF, Kilpatrick TJ (2002) LIF receptor signaling limits immune-mediated demyelination by enhancing oligodendrocyte survival. Nat Med 8(6):613–619

75. Kerr BJ, Patterson PH (2005) Leukemia inhibitory factor promotes oligodendrocyte survival after spinal cord injury. Glia 51(1):73–79, doi: 10.1002/glia.20177

76. Ishibashi T, Dakin KA, Stevens B, Lee PR, Kozlov SV, Stewart CL, Fields RD (2006) Astrocytes promote myelination in response to electrical impulses. Neuron 49(6):823–832

77. Laterza C, Merlini A, De Feo D, Ruffini F, Menon R, Onorati M, Fredrickx E, Muzio L, Lombardo A, Comi G, Quattrini A, Taveggia C, Farina C, Cattaneo E, Martino G (2013) iPSC-derived neural precursors exert a neuroprotective role in immune-mediated demyelination via the secretion of LIF. Nat Commun 4:2597, doi: 10.1038/ncomms3597

78. Chari DM (2007) Remyelination in multiple sclerosis. Int Rev Neurobiol 79:589–620, doi: 10.1016/s0074-7742(07)79026-8

79. Syed YA, Hand E, Mobius W, Zhao C, Hofer M, Nave KA, Kotter MR (2011) Inhibition of CNS remyelination by the presence of semaphorin 3A. J Neurosci 31(10):3719–3728, doi: 10.1523/jneurosci. 4930-10.2011

80. Beenken A, Mohammadi M (2009) The FGF family: biology, pathophysiology and therapy. Nat Rev Drug Discov 8(3):235–253, doi: 10.1038/nrd2792

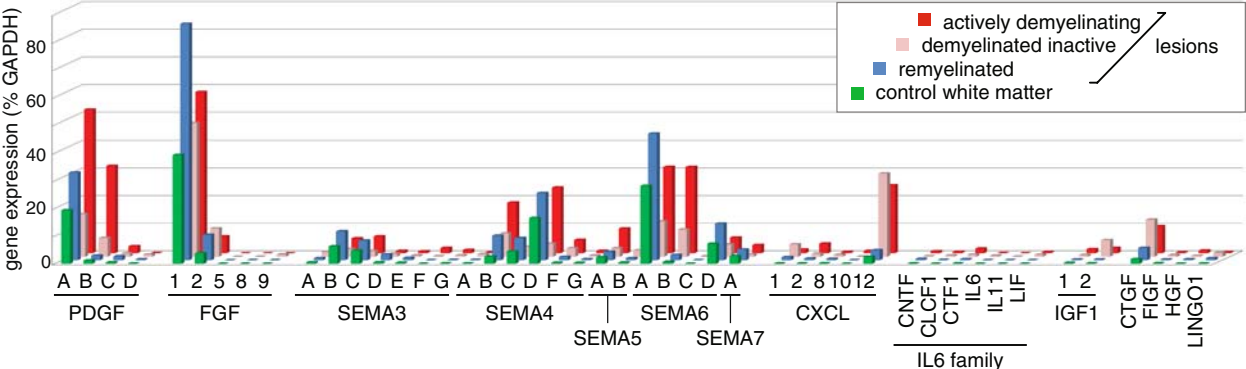
gene expression (% GAPDH)
0
20
40
60
80
actively demyelinating
demyelinated inactive
remyelinated
control white matter
lesions
A B C D
PDGF
1 2 5 8 9
FGF
A B C D E F G
SEMA3
A B C D F G
SEMA4
A B
SEMA5
A B C D
SEMA6
A
SEMA7
1 2 8 10 12
CXCL
CNTF
CLCF1
CTF1
IL6
IL11
LIF
IL6 family
1 2
IGF1
CTGF
FIGF
HGF
LINGO1

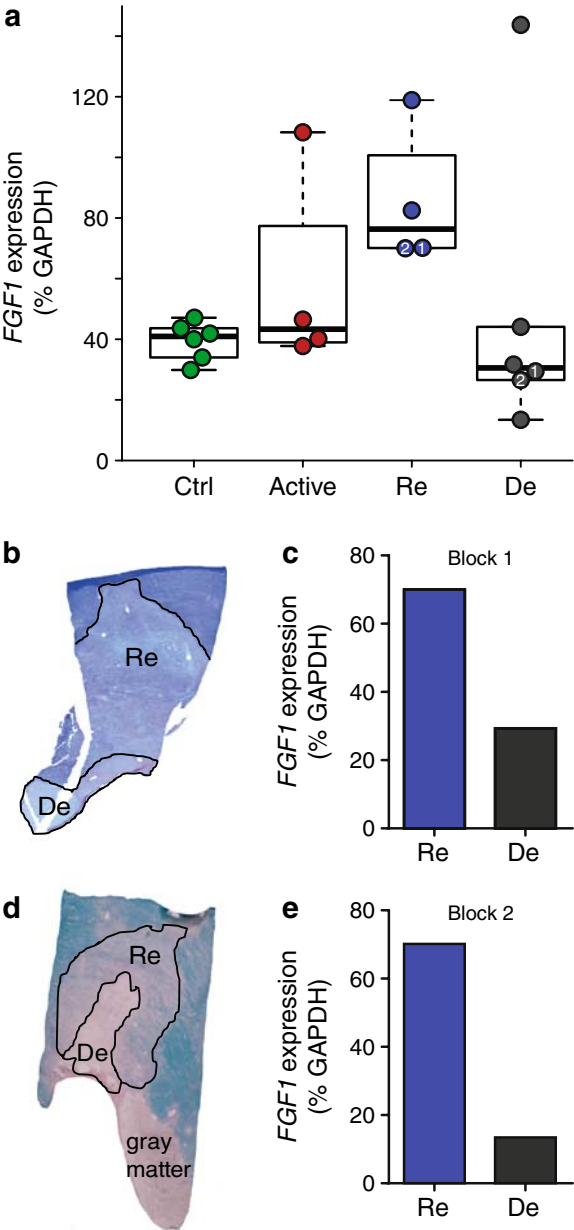
a
FGF1 expression (% GAPDH)
120
80
40
0
Ctrl
Active
Re
De
b
Re
De
c
Block 1
FGF1 expression (% GAPDH)
80
60
40
20
0
Re
De
d
Re
De
gray matter
e
Block 2
FGF1 expression (% GAPDH)
80
60
40
20
0
Re
De

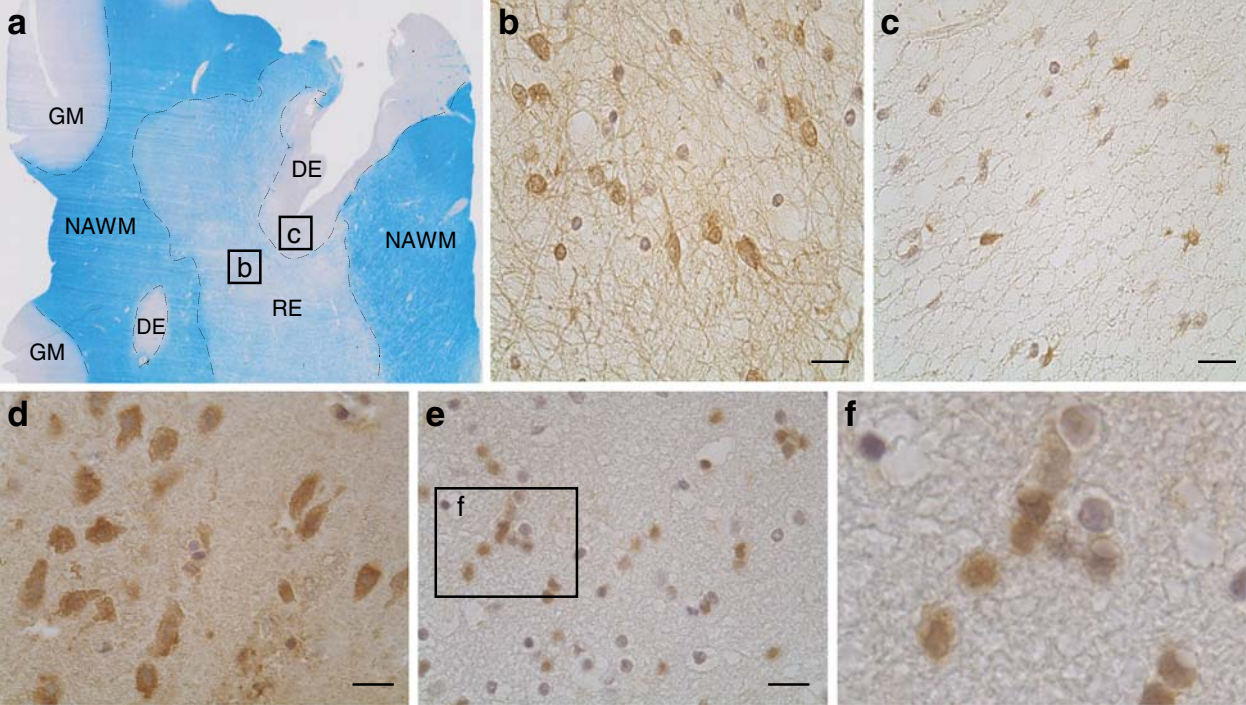
a
GM
NAWM
DE
c
b
NAWM
RE
DE
GM
b
c
d
e
f
f

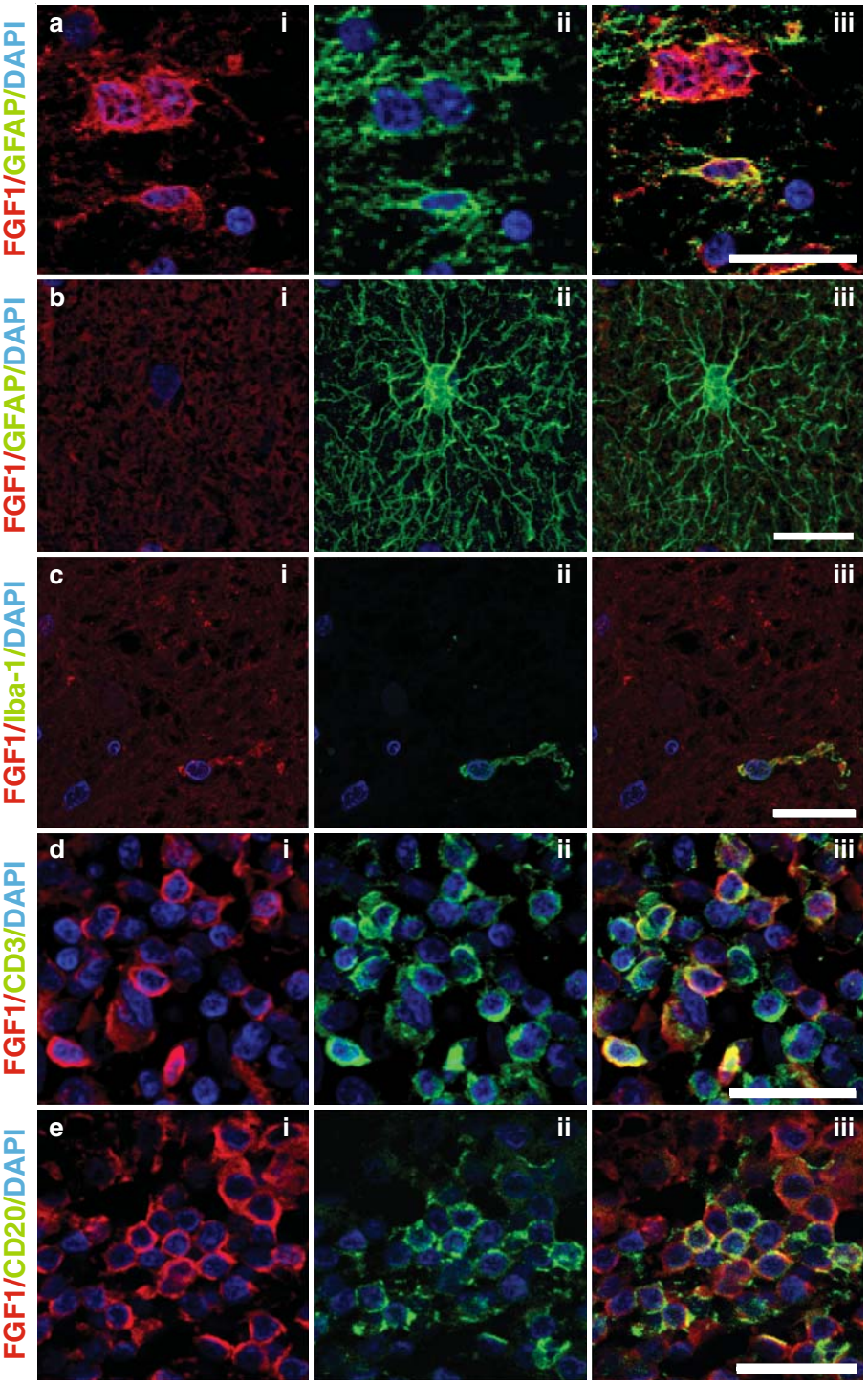
a
i
ii
iii
FGF1/GFAP/DAPI
b
i
ii
iii
FGF1/GFAP/DAPI
c
i
ii
iii
FGF1/Iba-1/DAPI
d
i
ii
iii
FGF1/CD3/DAPI
e
i
ii
iii
FGF1/CD20/DAPI

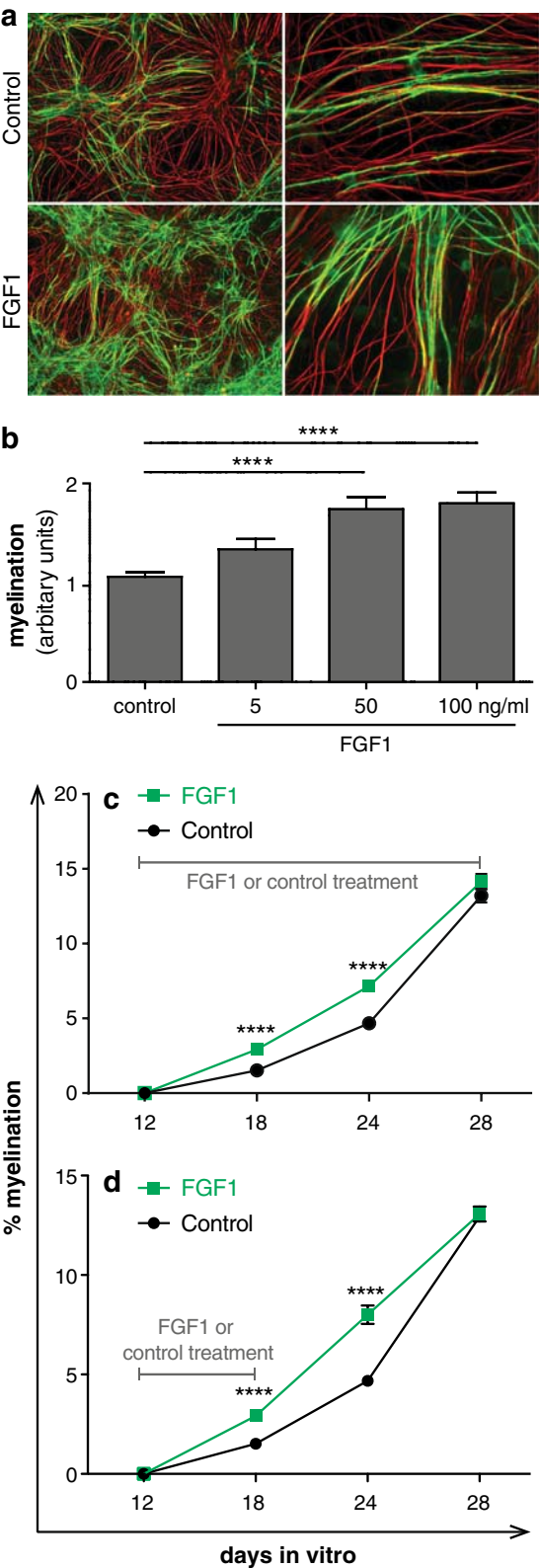
a
Control
FGF1
b
****
****
myelination
(arbitary units)
2
1
0
control
5
50
100 ng/ml
FGF1
c
FGF1
Control
FGF1 or control treatment
****
****
20
15
10
5
0
12
18
24
28
% myelination
d
FGF1
Control
FGF1 or
control treatment
****
****
15
10
5
0
12
18
24
28
days in vitro

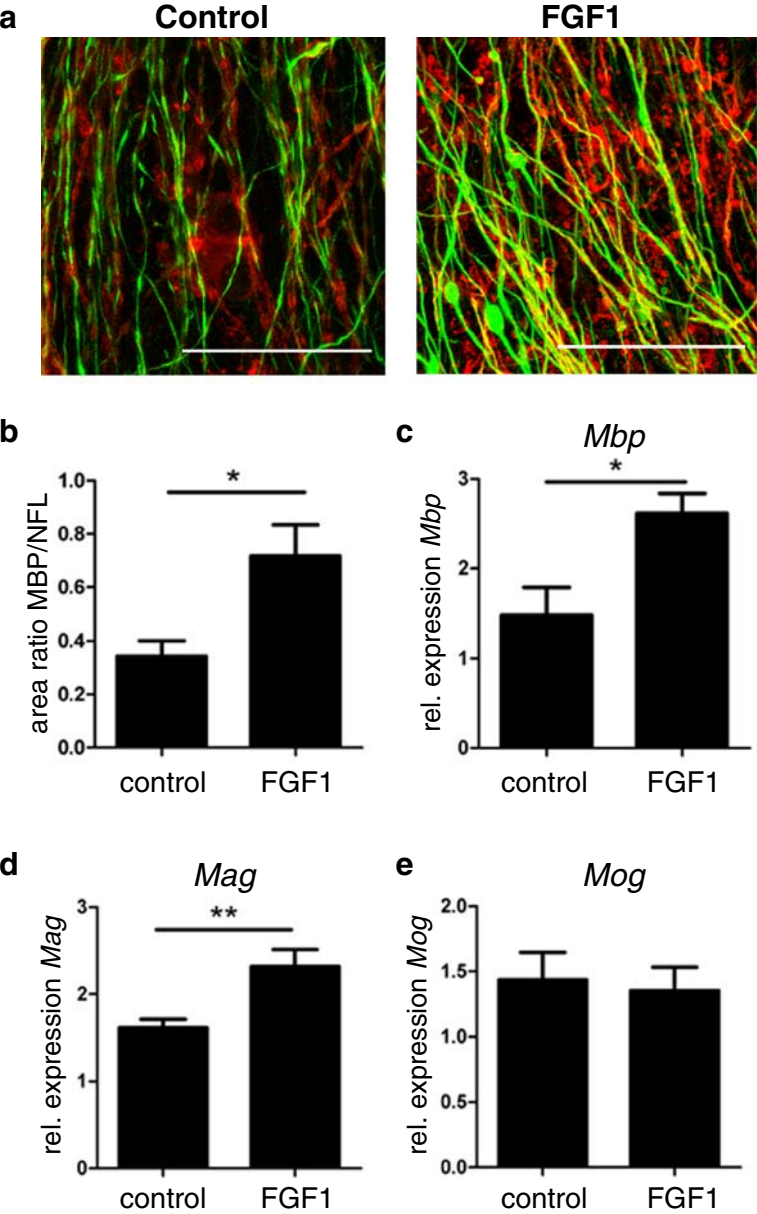
a
Control
FGF1
b
area ratio MBP/NFL
1.0
0.8
0.6
0.4
0.2
0.0
*
control
FGF1
c
Mbp
rel. expression Mbp
3
2
1
0
*
control
FGF1
d
Mag
rel. expression Mag
3
2
1
0
**
control
FGF1
e
Mog
rel. expression Mog
2.0
1.5
1.0
0.5
0.0
control
FGF1

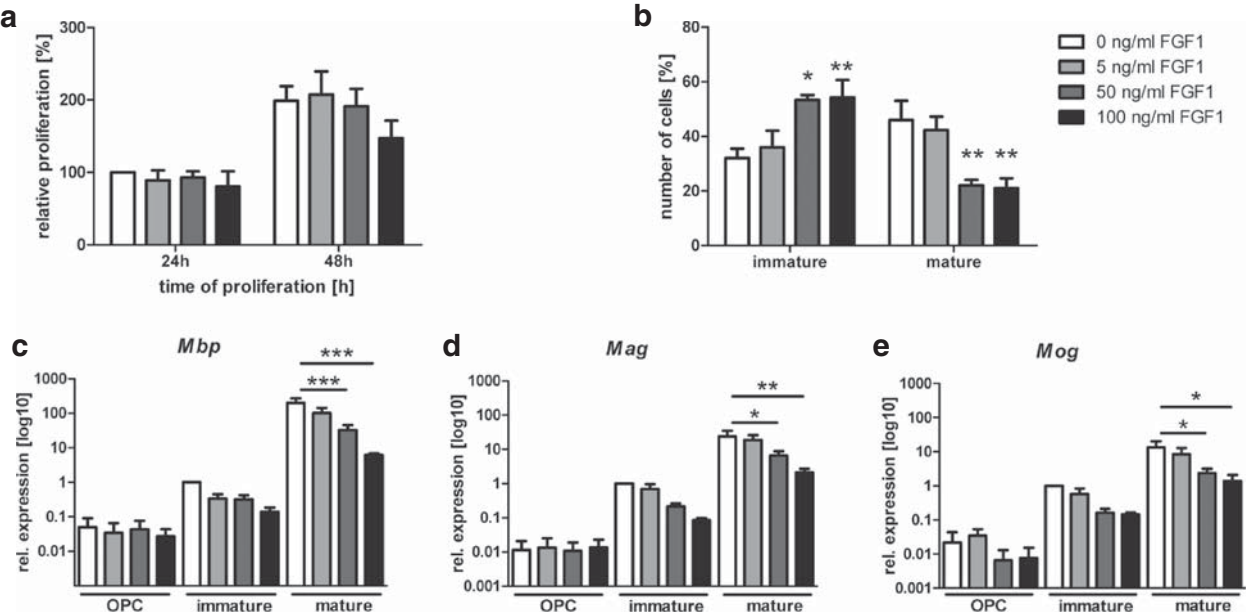
a
relative proliferation [%]
300
200
100
0
24h
48h
time of proliferation [h]
b
number of cells [%]
80
60
40
20
0
immature
mature
0 ng/ml FGF1
5 ng/ml FGF1
50 ng/ml FGF1
100 ng/ml FGF1
c
Mbp
rel. expression [log10]
1000
100
10
1
0.1
0.01
OPC
immature
mature
d
Mag
rel. expression [log10]
0.001
e
Mog

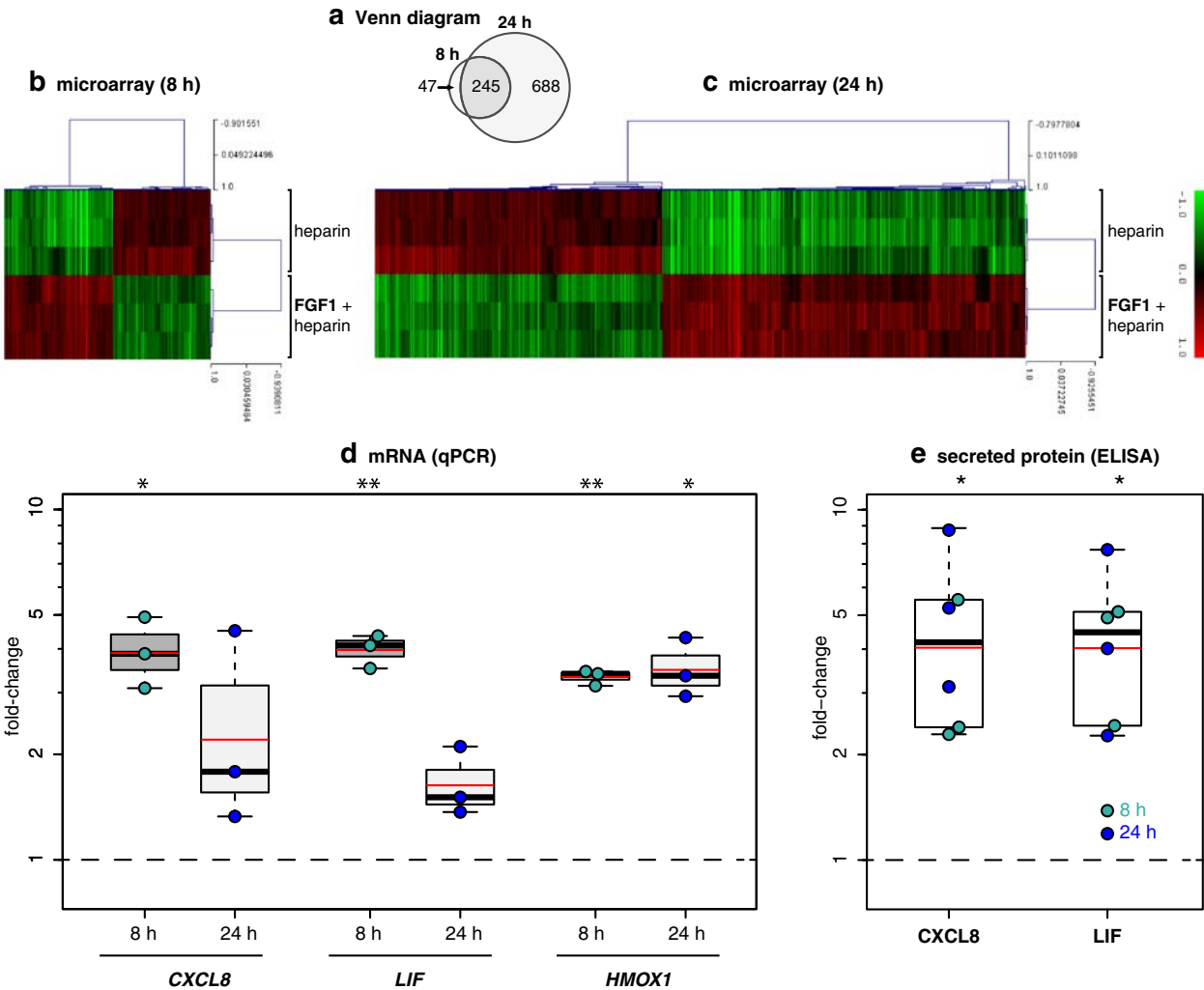
a Venn diagram
24 h
8 h
47
245
688
b microarray (8 h)
heparin
FGF1 + heparin
c microarray (24 h)
heparin
FGF1 + heparin
d mRNA (qPCR)
fold-change
8 h
24 h
CXCL8
LIF
HMOX1
e secreted protein (ELISA)
fold-change
8 h
24 h
CXCL8
LIF

Addtional files provided with this submission:

Additional file 1: Table S1. Frozen tissue samples used for qPCR and immunofluorescence (116k)
http://www.actaneurocomms.org/content/supplementary/s40478-014-0168-9-s1.pdf

Additional file 2: Figure S1. Unsupervised clustering reflects histological discrimination between remyelinated (blue) and demyelinated inactive (pink) lesion areas (125k)
http://www.actaneurocomms.org/content/supplementary/s40478-014-0168-9-s2.pdf

Additional file 3: Table S2. Expression levels of receptors and their fold changes in demyelinated inactive versus remyelinated lesions (29k)
http://www.actaneurocomms.org/content/supplementary/s40478-014-0168-9-s3.docx

Additional file 4: Figure S2. LRRN6A (LINGO-1) gene expression in different MS lesion types and control white matter (91k)
http://www.actaneurocomms.org/content/supplementary/s40478-014-0168-9-s4.pdf

Additional file 5: Table S3. Transcriptional changes induced by FGF1 in human primary astrocytes, after 8 and 24 h (34k)
http://www.actaneurocomms.org/content/supplementary/s40478-014-0168-9-s5.xlsx